



## 저작자표시-비영리-변경금지 2.0 대한민국

이용자는 아래의 조건을 따르는 경우에 한하여 자유롭게

- 이 저작물을 복제, 배포, 전송, 전시, 공연 및 방송할 수 있습니다.

다음과 같은 조건을 따라야 합니다:



저작자표시. 귀하는 원저작자를 표시하여야 합니다.



비영리. 귀하는 이 저작물을 영리 목적으로 이용할 수 없습니다.



변경금지. 귀하는 이 저작물을 개작, 변형 또는 가공할 수 없습니다.

- 귀하는, 이 저작물의 재이용이나 배포의 경우, 이 저작물에 적용된 이용허락조건을 명확하게 나타내어야 합니다.
- 저작권자로부터 별도의 허가를 받으면 이러한 조건들은 적용되지 않습니다.

저작권법에 따른 이용자의 권리는 위의 내용에 의하여 영향을 받지 않습니다.

이것은 [이용허락규약\(Legal Code\)](#)을 이해하기 쉽게 요약한 것입니다.

[Disclaimer](#)

공학석사학위논문

Investigation of New Iodinated  
Disinfection Byproducts Formation  
from Imidazole Compounds during  
Chlorination for Sustainable and  
Safe Water Management

2022년 8월

서울대학교 대학원  
건설환경공학부  
최 서 영

# Investigation of New Iodinated Disinfection Byproducts Formation from Imidazole Compounds during Chlorination for Sustainable and Safe Water Management

지도 교수 최 정 권

이 논문을 공학석사 학위논문으로 제출함  
2022년 8월

서울대학교 대학원  
건설환경공학부  
최 서 영

최서영의 공학석사 학위논문을 인준함  
2022년 6월

위 원 장	남 경 필	(인)
부위원장	최 정 권	(인)
위 원	최 용 주	(인)

# Abstract

Imidazoles are often found in drinking water sources as constituents of biological substances (e.g., histidine, histamine, and nucleic acid) as well as man-made chemicals such as pharmaceutical compounds and pesticides. Because imidazoles are polar aromatic compounds, they have a high potential for halogenation, and thus could be important precursors of iodinated disinfection by-products (I-DBPs). As the formation of I-DBPs in drinking water becomes a growing concern due to their high toxicity compared to Cl- and Br-DBPs, there is a need to investigate this possibility.

This study was conducted to identify the formation potentials for iodinated imidazole DBPs from three imidazole organic compounds: imidazole-carboxylic acid, phenyl-imidazole-carboxylic acid, and histidine. Using liquid chromatography-mass spectrometry (LC-MS) analysis, iodinated imidazole DBPs were detected in laboratory simulated chlorinated water as well as their structures were proposed. Imidazole-carboxylic acid produced di-I- and tri-I-imidazole and phenyl-imidazole-carboxylic acid formed mono-I- and di-I-phenyl imidazole in which the iodine substitution was presumed to have occurred on the benzene ring. While histidine was conducted in a N-tert-Butyloxycarbonyl group (N-BOC group) protected form to inactivate the free amine group to the electrophilic reaction. N-BOC-His produced N-BOC-I- and N-BOC-di-I-His.

We focused on the dominant iodinated DBPs formed from histidine. For iodinated histidine compounds, we synthesized these compounds to quantify their yields. This study demonstrated that histidine is more reactive during the chlorination in the presence of iodide than only chlorine exists. The influence of disinfection

conditions such as NaOCl dose, as well as water conditions (e.g., pH,  $I^-$  concentrations, and  $Br^-/I^-$  ratio) on the degradation of histidine and the formation of I-DBPs, were also investigated. Large decomposition of histidine and high formation of iodinated histidine products were generated at lower NaOCl dose,  $Br^-/I^-$  ratio, and higher  $I^-$  concentration. I-DBPs yield was significantly affected by solution pH. A high concentration of iodinated histidine DBPs was produced under alkaline conditions. Finally, we compared yields of iodinated histidine DBPs with THMs and HAAs formed simultaneously from the chlorination of histidine. The maximum total yield of THM and HAA was less than 0.4% and it was very small compared to the yield of iodinated histidine products (maximum ~5.5%). These findings support that the form of the iodinated histidine compounds may play a more important role than the currently regulated THMs or HAAs in terms of production amount. However, the evidence for this should be supported by further toxicological studies on the structure and epidemiology of these compounds.

**Keyword : Chlorine disinfection; Iodide; Imidazole; Histidine; DBPs**  
**Student Number : 2020-27348**

# Table of Contents

Chapter 1. Introduction .....	1
1.1. Study Background .....	1
1.2. Purpose of Research .....	4
Chapter 2. Materials and Methods .....	5
2.1. Chemicals and Materials .....	5
2.2. Methods .....	7
2.2.1. Chlorination of Imidazole Compounds in the Presence of $I^-$ .....	7
2.2.2. Chlorination of Histidine in the Various Conditions .....	8
2.2.3. THMs and HAAs Formation from the Chlorination of Histidine .....	10
2.2.4. Synthesis of Iodinated Histidine Products .....	11
2.3. Analysis .....	15
2.3.1. LC-MS and LC-QTOF-MS/MS Analysis .....	15
2.3.2. GC-MS Analysis .....	17
2.3.3. $^1H$ -NMR Analysis and Results .....	18
Chapter 3. Results and Discussion .....	20
3.1. Identification of Iodinated Byproducts from Imidazole .....	

Compounds during Chlorination with Iodide-Containing Water.....	20
3.1.1. Imidazole-Carboxylic Acid.....	20
3.1.2. Phenyl-Imidazole-Carboxylic Acid.....	24
3.1.3. Histidine.....	27
3.2. Kinetics Study of Histidine Reactivity and Iodinated Byproducts Formation .....	31
3.3. Factors Influencing Histidine Degradation and Iodinated Histidine Products Formation .....	33
3.3.1. Chlorine Dose .....	33
3.3.2. Iodide Concentration .....	35
3.3.3. Bromide/Iodide Molar Ratio .....	37
3.3.4. pH of Solution.....	39
3.4. Comparison of Yields of Iodinated Histidine Products with Other Regulated DBPs (THMs and HAAs) .....	41
 Chapter 4. Conclusion .....	 44
 Reference .....	 48
 Abstract in Korean.....	 53

## List of Tables

<b>Table 1.</b> Three model imidazole compounds .....	<b>7</b>
<b>Table 2.</b> THMs and HAAs method information for retention time (min) and selected ion (m/z) .....	<b>17</b>



# List of Figures

<b>Figure 1.</b> The classificaion of the organic DBPs.....	3
<b>Figure 2.</b> Structure of a imidazole ring .....	4
<b>Figure 3.</b> Scheme of research.....	5
<b>Figure 4.</b> Chlorine disinfection process .....	9
<b>Figure 5.</b> Thin-layer-chromatography (TLC) .....	13
<b>Figure 6.</b> Schematic summarizing the synthesis process .....	14
<b>Figure 7.</b> $^1\text{H}$ NMR spectra of (a) N-BOC-L-histidine (b) N-BOC-5-iodo-L-histidine (c) N-BOC-2,5-iodo-L-histidine.....	18
<b>Figure 8.</b> LC/(+)ESI-MS TIC chromatograms of imidazole-carboxylic acid .....	21
<b>Figure 9.</b> Proposed structures of (a) di-I-imidazole (b) tri-I-imidazole .....	23
<b>Figure 10.</b> LC/(+)ESI-MS TIC chromatograms of phenyl-imidazole-carboxylic acid .....	24
<b>Figure 11.</b> Proposed structures of (a) I-phenyl-imidazole (b) di-I-phenyl-imidazole .....	26
<b>Figure 12.</b> LC/(+)ESI-MS TIC chromatograms of N-BOC-histidine and mass spectra.....	28
<b>Figure 13.</b> LC-QTOF-MS/MS mass spectra .....	29
<b>Figure 14.</b> Proposed structures of (a) N-BOC-Cl-histidine (b) N-BOC-I-histidine (c) N-BOC-di-I-histidine.....	30
<b>Figure 15.</b> (a) the degradation of histidine and (b) the formation of iodinated histidine products as a function of reaction time (hr) ...	31
<b>Figure 16.</b> Effect of initial NaOCl dose .....	33
<b>Figure 17.</b> Effect of $\text{I}^-$ concentration.....	35
<b>Figure 18.</b> Effect of $\text{Br}^-/\text{I}^-$ molar ratio .....	37

<b>Figure 19.</b> Effect of pH .....	<b>39</b>
<b>Figure 20.</b> Effect of $I^-$ concentration and chlorine reaction time on the formation of THMs and HAAs during chlorination of histidine	<b>41</b>
<b>Figure 21.</b> Comparison of molar yields of iodinated histidine products with THMs and HAAs formed after 24 h chlorination	<b>.43</b>

# Chapter 1. Introduction

## 1.1. Study Background

The supply of safe drinking water to ensure the quality of life and to lead a healthy life has always been treated as an important issue. Biological safety of drinking water has been ensured by disinfection that inactivates disease-causing organisms and prevents the transmission of potentially fatal waterborne disease. Chlorine is the most widely used disinfectant in U.S. and Korea, because it is cost-effective and has a long-lasting residues in distribution systems.<sup>1,2</sup> However, chlorine inevitably reacts with dissolved organic matter present in the raw water to form disinfection by-products (DBPs) that are potentially hazardous to human health.

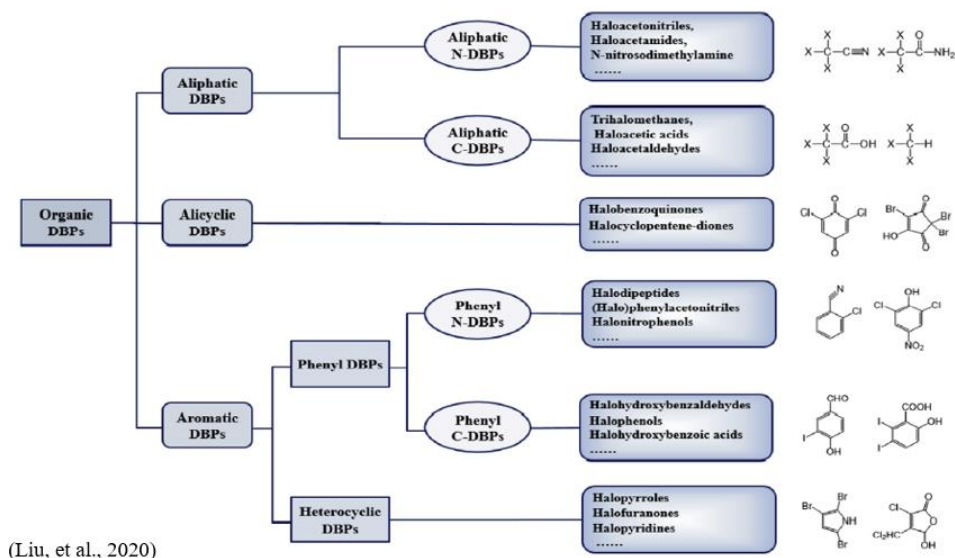
Since trihalomethanes (THMs) were first discovered as DBPs in chlorinated drinking water in 1974,<sup>3</sup> the formation of various groups of DBPs, such as haloacetic acids (HAAs), haloacetonitriles (HANs), and halonitromethanes (HNMs), etc., has been revealed.<sup>4,5</sup> So far, over 700 DBPs have been identified, while only a small fraction, 11 DBPs including 4 trihalomethanes, 5 haloacetic acids, bromate, and chlorite have been regulated. Despite several years of efforts to find new DBPs, the known halogenated DBPs only account for approximately 30% of the total organic halogen (TOX) content.<sup>5</sup>

In the source water, iodide is often present naturally by the salt water intrusion, leaching from watershed rocks or soils, and decomposition of organic matters.<sup>6</sup> The concentration of iodide also can be elevated by the anthropogenic sources such as wastewater discharge.<sup>38</sup> *Richardson et al., (2008)* reported concentrations of  $I^-$  0.4–104  $\mu g L^{-1}$  in the source of drinking water treatment plants (DWTPs in 22 cities of USA and 1 of Canada).<sup>24</sup>

Chlorination could oxidize iodide dissolving in the water into reactive hypoiodous acid (HOI) which is the most reactive iodine species, and the reaction of HOI with NOM can form iodinated DBPs (I-DBPs). In fact, there are cases where I-DBPs have been detected even in actual drinking water. For example, the median concentration of I-THMs detected from the 12 DWTPs was  $2.0 \mu\text{g L}^{-1}$ , and that of I-HAAs was  $1.44 \mu\text{g L}^{-1}$  in drinking water from 23 cities in the U.S.<sup>24</sup> In Korea,  $0.12 \pm 0.19 \mu\text{M}$  of I-THM was detected in 70 water purification plants, and it was affected by the disinfection system, region, season and water source.<sup>43</sup> Moreover, due to the more cytotoxicity and genotoxicity of I-DBPs than their brominated and chlorinated analogues despite its low concentration.<sup>7,8,9</sup> For example iodoacetic acid has been shown to induce the most mutagenic potency in *S.typhimurium* and express the highest genotoxicity in CHO cells among the haloacetic acids analyzed. The cytotoxicity and genotoxicity of the haloacetic acids were related to cellular uptake, transport and subsequent chemical interactions with cellular macromolecules due to the lipophilicity and degree of ionization-dependent transport mechanism of the chemical.<sup>7</sup> Therefore, concerns about the unknown iodinated DBP have recently attracted increased attention.

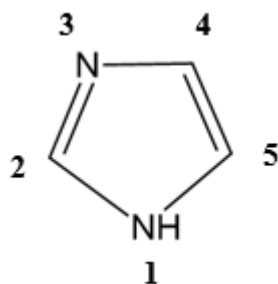
Aromatic DBP refers to DBPs with planar ring structures following Hückel's rule involving phenyl or heterocyclic structures. These aromatic structures have properties that provide increased stability or high reactivity to electrophilic substitutions.<sup>10</sup> This suggests that iodide substitution in the aromatic structure may lead to the formation of other toxic I-DBPs, and further decomposition to produce aliphatic DBPs with lower molecular weight.<sup>11</sup> So far, the large groups of aromatic DBPs with benzene or phenolic properties, such as halophenole (HPs), halonitrophenols (HNPs) and halohydroxybenzaldehydes (HBADs), have been previously studied. However, despite the many types of heterocyclic structures, compared to phenyl structure, far fewer studies have reported on

the heterocyclic structures as precursors. It suggests that there are an infinite number of heterocyclic DBPs that have not yet been discovered.



▲ Figure 1. The classification of the organic DBPs.

In this study, we selected imidazole compounds from among various heterocyclic structures for chlorination target material. Imidazoles are often found in drinking water sources as not only constituents of biological substances, including histidine, histamine, and nucleic acid, but also pharmaceutical compounds. Imidazole is a planar five-membered ring system with three carbon and two nitrogen atom in 1 and 3 positions, as shown in Figure 2. Imidazole is amphoteric in nature, susceptible to electrophiles and nucleophilic attack. It indicates that imidazole compounds can acts as a precursor of I-DBPs by participating in the iodine substitution reaction during chlorination in the presence of iodide. Besides Imidazole and its derivatives could have biological activities considered as possible antimicrobial, anticancer, analgesic activities, etc.<sup>12</sup> Thus, I-DBPs formed from imidazole compounds may have novel toxicity, and further in vivo assays or epidemiology studies associated with adverse health effects should be conducted on this evidence.



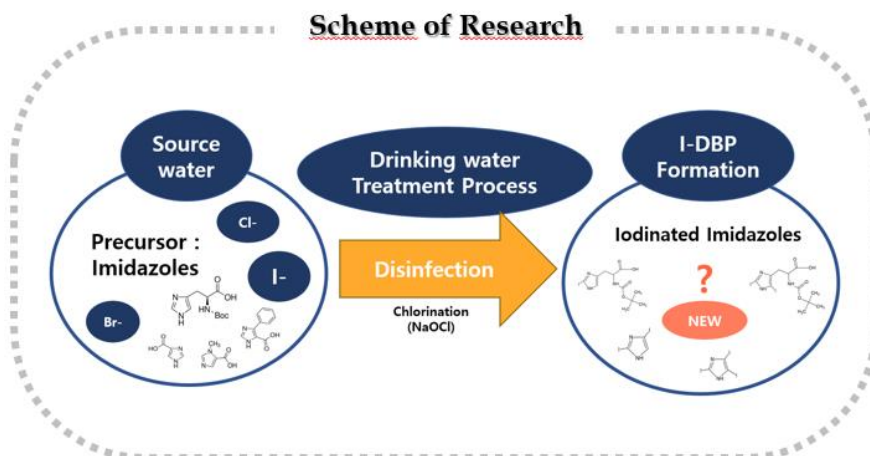
▲ **Figure 2.** Structure of a imidazole ring.

Among imidazole compounds, the chlorination experiments in this study, we used imidazole-carboxylic acid, phenyl-imidazole-carboxylic acid, and histidine. Also histidine was selected as a representative imidazole compound to assess the effects of various solution conditions on the formation iodinated imidazole DBPs. Because histidine, which is 1 of the essential amino acid, contained in urine, sweat, and personal care products, has been detected as one of the abundant amino acids in nature water and revealed that most reactive with chlorine.<sup>13</sup> The  $\alpha$ -amino group of free histidine is highly reactive with the electrophile, but the use of protecting group of the amino group triggers an amide bond, inactivating the  $\alpha$ -amino group from the reaction with the electrophile. Thus, we used N-tert-Butyloxycarbonyl histidine (N-BOC-His) to prevent the iodination of  $\alpha$ -amino group, and to report only the reactivity of the imidazole ring with HOI.

## 1.2. Purpose of Research

The ultimate purpose of this study is to determine whether imidazole serves as a precursor of iodinated DBPs during chlorination in the presence of iodide. To achieve this purpose, several specific objectives were set up for this study.

- (1) Identify the newly formed iodinated DBPs from the respective precursor, imidazole-carboxylic acid, phenyl-imidazole-carboxylic acid, and histidine, in the iodide-containing chlorinated water.
- (2) Investigate how the presence of iodide during chlorine disinfection can influence the degradation kinetics of histidine and formation kinetics of iodinated histidine products.
- (3) Assess the influence of disinfection conditions such as NaOCl dose,  $I^-$  concentration,  $Br^-/I^-$  molar ratio, and pH on histidine reactivity to iodine substitution.
- (4) Compare the yields of these iodinated histidine DBPs with those of THMs and HAAs, which are the main groups of DBPs.



▲ Figure 3. Scheme of research

# Chapter 2. Materials and Methods

## 2.1. Chemicals and Materials

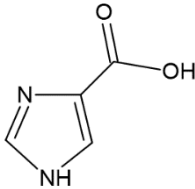
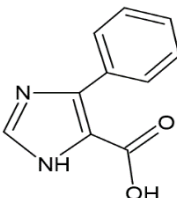
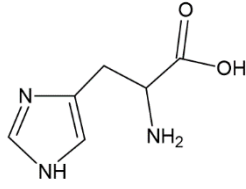
N-BOC-L-histidine (N-BOC-His; 99+%), sodium hypochlorite (NaOCl; 5.65~6%, w/v), potassium iodide (KI; 99+%), iodine (I<sub>2</sub>; 0.1N standardized solution) and L-ascorbic acid (99+%) were purchased from Alfa Aesar. 4-imidazole-carboxylic acid (Imi-COOH; 99+%), 4-phenyl-1H-imidazole-5-carboxylic acid (Phe-Imi-COOH; 99+%), a standard mixture of four regulated THMs (200  $\mu\text{g/mL}$  of each component in methanol) including bromodichloromethane (CHCl<sub>2</sub>Br), tribromomethane (CHBr<sub>3</sub>), trichloromethane (CHCl<sub>3</sub>) and dibromochloromethane (CHClBr<sub>2</sub>), a standard mixture of nine HAAs (200  $\mu\text{g/mL}$  of each component in methyl tert-butyl ether) including bromoacetic acid (MBAA), bromochloroacetic acid (BCAA), bromodichloroacetic acid (BDCAA), chloroacetic acid (MCAA), dibromochloroacetic acid (DBCAA), dibromoacetic acid (DBAA), dichloroacetic acid (DCAA), tribromoacetic acid (TBAA) and trichloroacetic acid (TCAA), individual standards of triiodomethane (CHI<sub>3</sub>) and iodoacetic acid (MIAA), and sodium bromide (NaBr; 99+%) were purchased from Sigma-Aldrich. Individual I-THMs including chlorodiiodomethane (CHClI<sub>2</sub>) and dichloroiodomethane (CHCl<sub>2</sub>I), and I-HAAs including diiodoacetic acid (DIAA) and chloroiodoacetic acid (CIAA) were purchased from CanSyn Chem. Co. (New Westminster, BC, Canada). All reagent-grade chemicals were used without further purification. A stock of free chlorine (HOCl) solution was prepared from sodium hypochlorite (NaOCl, 5.65~6% w/v) and then diluted with Milli-Q pure(deionized) water. The concentration of free chlorine was standardized using UV-vis spectrophotometry at 292nm (362 M<sup>-1</sup>cm<sup>-1</sup> <sup>14</sup>) and measured to be 860mM. All experiments were conducted using deionized water (DIW, 18.2 M $\Omega$ cm, Milli-Q System, France).



## 2.2. Methods

### 2.2.1. Chlorination of Imidazole Compounds in the Presence of I<sup>-</sup>

All disinfection experiments in this study were performed in 120mL glass bottles with a batch system and conducted in triplicate. The pH of aqueous solutions was adjusted to  $7.0 \pm 0.1$  with 50 mM of the phosphate-buffered solution. Imidazole-carboxylic acid, phenyl-imidazole-carboxylic acid, and histidine were selected as model precursors, and both of them have an imidazole moiety. Each sample was prepared by dissolving each compound (50  $\mu$ M) and KI (0–100  $\mu$ M) in a 100 mL of buffered solution. Then NaOCl (100  $\mu$ M) was added to water samples with a molar ratio of 2:1 to each imidazole-precursor. Because HOI is not stable in water, it was freshly produced directly by adding free chlorine in the condition (each model solutions) of containing iodide.<sup>15</sup> The reaction mixtures were sealed and mixed well for 24 h in the dark at room temperature. After the 24 h reaction, the reactive oxidants residue (free chlorine and free iodine species) in aqueous solution was quenched by addition of ascorbic acid at 1.5 times the molar concentration of total oxidants applied.

	Imidazole-carboxylic acid	Phenyl-imidazole-carboxylic acid	N-BOC-L-histidine
Structure			
Formula	C <sub>4</sub> H <sub>4</sub> N <sub>2</sub> O <sub>2</sub>	C <sub>10</sub> H <sub>8</sub> N <sub>2</sub> O <sub>2</sub>	C <sub>11</sub> H <sub>16</sub> N <sub>3</sub> O <sub>4</sub>
MW	112.03	188.06	256.12

▲ Table 1. Three model imidazole compounds

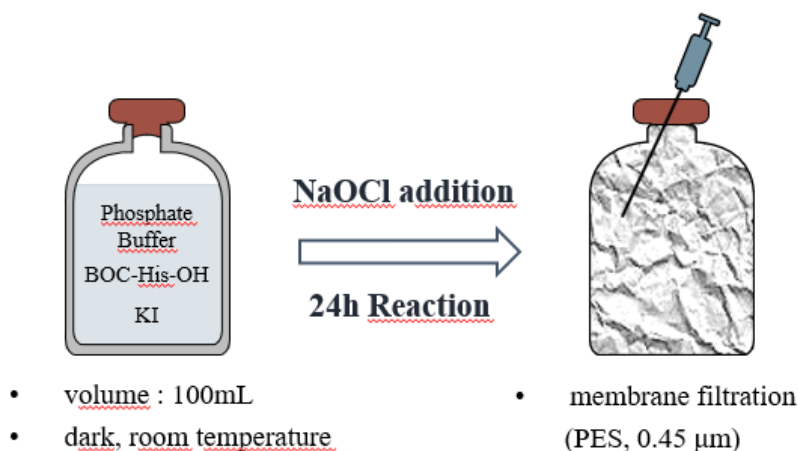
## 2.2.2. Chlorination of Histidine in the Various Conditions

To investigate the various effects on the reactivity of histidine and the formation of iodinated histidine products during chlorination, additional chlorine experiments were performed in the presence of iodide. The chlorination process was similar to above 2.2.1.: All experiments were conducted in a batch reactor and triplicated within pH 7. Sample was prepared by dissolving N-BOC-His (5  $\mu$ M) and KI (0–10  $\mu$ M) in a 100 mL of buffered solution. Then NaOCl (10  $\mu$ M) was added at a molar ratio  $[\text{HOCl}/\text{OCl}^-]:[\text{AA}]=2:1$ . The reaction mixtures were sealed and mixed well for 24 h in the dark at room temperature. After the 24 h reaction, the reaction was quenched by addition of ascorbic acid at 1.5 times the molar concentration of total oxidants applied. As ascorbic acid reduces halogenated amine groups (i.e., N-X, where X = Cl, Br, or I) to N-H bonds, but does not affect the C-X bond on the side chain, ascorbic acid was added to quench the residual HOCl or HOI and revert any N-X bond back to N-H bond.<sup>16,17,18</sup> This supports the identification of more stable byproducts halogenated on the carbon group under chlorination conditions.

The kinetic experiments were performed to monitor the degradation(disappearance) of the N-BOC-His and the formation of iodinated byproducts. At evenly spaced time intervals (0, 3, 10, 30, 45, 60 min (1 h), 2, 4, 6, 12, and 24 h), 2mL aliquots of the reaction mixture were removed, and each aliquot was quenched with excess of ascorbic acid.

Similar experimental procedures were adopted when investigating the effects of chlorination conditions (etc., as a function of NaOCl dose, I- concentration, Br- concentration, pH) on the degradation of histidine and the formation of byproducts. The free chlorine was applied at a molar ratio of 0 to 10 related to initial histidine, in the

range of NaOCl 0–50  $\mu$ M. Five initial iodide ion concentrations (0, 0.5, 2.5, 5, and 10  $\mu$ M) and bromide ion concentrations (0, 10, 25, 50 and 100  $\mu$ M) were injected in each experiment. For the effect of solution pH, the chlorination was conducted at pH ranging from 5 to 9 by adjusting the pH of a phosphate–buffered solution using sulfuric acid or sodium hydroxide.



▲ **Figure 4.** Chlorine disinfection process

### 2.2.3. THMs and HAAs Formation from the Chlorination of Histidine

In order to investigate the formation of chlorinated or iodinated trihalomethanes (THMs) and haloacetic acids (HAAs) from chlorinated water samples, the experiments were conducted as follows: the initial concentration of N-BOC-His of 50  $\mu$ M in the phosphate buffer, pH 7, reacted with NaOCl of 100  $\mu$ M, with  $I^-$  concentration of 0–100  $\mu$ M. All reactions were performed at dark and room temperature of 23  $^{\circ}$ C. After 24 hours, the reaction was quenched with an ascorbic acid solution (1.5 times of total oxidant concentration) immediately to prevent potential hydrolytic loss of byproducts due to remaining oxidants. Then, 50 mL of water samples were used to liquid–liquid extraction (LLE) procedure.

The LLE for trihalomethanes (THMs, including  $CHCl_3$ ,  $CHCl_2I$ ,  $CHClI_2$ , and  $CHI_3$ ) was performed similarly to that described in USEPA Method 511.1.<sup>19</sup> Briefly, 3 mL of MTBE and 10 g of  $Na_2SO_4$  were injected into a 50 mL chlorinated water sample. The tightly sealed bottle was shaken vigorously for 2 min, and then, 1 mL of extract was transferred to a 1.5-mL chromatographic vial and stored at  $-20^{\circ}$ C.

Haloacetic acids (HAAs, including  $CH_2ClCOOH$  (MCAA),  $CHCl_2COOH$  (DCAA),  $CCl_3COOH$  (TCAA),  $CHClI_2COOH$  (CIAA),  $CH_2ICOOH$  (MIAA), and  $CHI_2COOH$  (DIAA)) were determined using the USEPA Method 522.2.<sup>20</sup> Briefly, a 50 mL water sample was acidified with concentrated  $H_2SO_4$  to pH < 5. After that, 10 g of  $Na_2SO_4$  was added for saturation, and a water sample was extracted with 4 mL of MTBE. 2 mL aliquot of MTBE was separated and methylated by adding 1 mL of 10%  $H_2SO_4$ /methanol solution and kept at 50  $^{\circ}$ C for 2 h. Then the extract was neutralized with 4 mL of  $NaHCO_3$ . The 1 mL of the concentrate in MTBE was transferred to a chromatographic vial and stored at  $-20^{\circ}$ C.

## 2.2.4. Synthesis of Iodinated Histidine Products

To determine the yields of new I-DBPs from histidine after chlorination, BOC-5-iodo-histidine and BOC-2,5-diiodo-histidine were synthesized by modifying Brunings' method.<sup>21</sup> Since the iodination of the imidazole ring slowed as the acidity of the solution increased,<sup>22</sup> the reaction was carried out under alkaline conditions. Separation of the synthetic compounds was performed by column chromatography, and the progress was confirmed through TLC analysis. TLC analysis was performed on silica gel 60 (230–450 mesh, Alfa Aesar) and spots were visualized by spraying ninhydrin solution. To identify the structures of the synthesized iodinated N-BOC-histidines, <sup>1</sup>H-NMR analysis was further performed using a 300 MHz AVANCE III HD (Bruker, German) spectrometer equipped with a <sup>1</sup>H 5-mm probe and TopSpin 3.X software.

### (1) Protocol for the iodination step :

A solution of 0.5 g of N-BOC-L-Histidine in 100 mL of 0.25 N NaOH and 50 mL of n-Hexane (n-C<sub>6</sub>H<sub>14</sub>) was placed in a 300 mL Erlenmeyer flask and cooled in an ice-water bath. An iodine-hexane solution, dissolved in 0.83 g of I<sub>2</sub> in 150 mL of n-Hexane, was added dropwise with vigorous stirring over 90 min. As the iodine-hexane solution was excessively emulsified, the mixture gradually became purple. After the addition was complete and stirred for additional minutes, 0.56 g of KIO<sub>3</sub>, dissolved in 20 mL of deionized water and 10 mL of concentrated HCl, was added. Then, add pure n-hexane, close the lid, and shake vigorously. In this process, the iodide ion residual, present at the minimum allowed by the substitution reaction, is converted to iodine as potassium iodate and acid are added and moved to the organic solvent layer. The mixture was allowed to separate the two layers (the aqueous layer and the hexane layer) and then removed the iodine-hexane layer. This extraction with hexane process was repeated three times. The

remaining solution was concentrated to dryness in a vacuum at 35 °C. About 1 g of an amorphous brown solid in a mixed state of His, I-His, and di-I-His in which the amine group of  $\alpha$ -carbon was protected by the BOC group was obtained. The dried product was stored at 4 °C in an air-tight container.

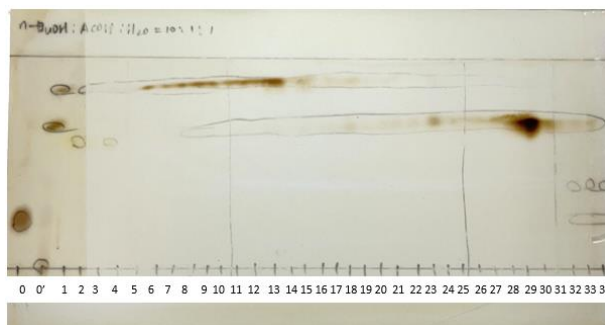
## **(2) Protocol for the separation and purification step :**

Chromatographic method using a column with silica gel 60 (200–400 mesh) was performed to separate the mixed product into their individual constituents and remove side products. A chromatography column ( $\phi$  14.4 × 1.8t × h400mm, 70mL) equipped with a filter to prevent sand and silica from flowing down from the bottom was used. Silica gel dissolved in a developing solvent in which dichloromethane and methanol were mixed in a ratio of 5:1 (v/v) was added to the top of the filter while flowing, and the surface was flattened. Then I added a layer of sand on top to avoid mixing the silica underneath by adding the sample and solvent later. The column was prepared by continuously flowing the solvent to prevent the column from drying and cracking in the adsorbent. The synthesized mixture to be purified was then dissolved in a small amount of a developing solvent and carefully added to the top of the silica gel. The column was developed with a solvent gradient from 5:1 to 5:7 (v/v) using dichloromethane and methanol of different polarities. Dichloromethane, a relatively less polar solvent, binds the compound to the stationary phase, causing slow elution. Therefore, increasing the proportion of methanol, a highly polar solvent, allowed the polar compound to enter the mobile phase rapidly, resulting in faster elution and increased travel distance. In addition, to accelerate the solvent flow, compressed air was used to drive the solvent through the column. The separation of the compounds was achieved by collecting the eluent from the bottom of the column. The elution sequence in a mixture depends on the polarity of the substances and passes through the column in

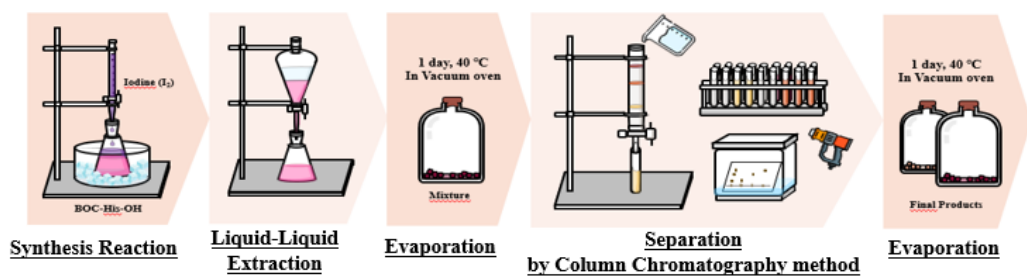
order of low polarity to high polarity. Therefore, it was eluted in the order from N-BOC-di-I-His to N-BOC-mono-I-His.

### (3) TLC analysis :

The success of the separation during the process and the selection of eluent containing the isolated compound were determined by spotting the fractions on TLC. Silica gel 60 plates (230–450 mesh, Alfa Aesar) were used, and ten microliters of each fraction collected from column chromatography along with the initial mixture were loaded to the marked points about 1 cm from the bottom of the plate. The plates were developed in n-butanol:acetic acid:water=10:1:1 (v/v/v) and spots were visualized by spraying ninhydrin solution, which was suitable for selectively staining amino acids and possible permanent visualization in red. Fraction no.0 was original N-BOC-His, 0' was a mixture of the synthesized compounds, and fractions no.1–34 were collected eluent from column chromatography in order. To increase the purity of each substance, fraction numbers that do not exist in a mixed state were selected and divided into two compartments: fraction no.5–10 of N-BOC-di-I-His and fraction no.26–30 of N-BOC -I-His.



▲ **Figure 5.** Thin-layer-chromatography (TLC): N-BOC-Histidine standard (0), synthesized mixture (0' ) and eluted fractions from column chromatography (from 1 to 34)



▲ Figure 6. Schematic summarizing the synthesis process.



## 2.3. Analysis

### 2.3.1. LC–MS and LC–QTOF–MS/MS Analysis

For identification of the iodinated byproducts formed by chlorination of imidazole compounds with iodide and quantification of N–BOC–His loss or iodinated byproducts yield, a Single quadrupole liquid chromatography mass spectrometry (LC–MS) (Agilent 6120DW, USA) were used. The LC system (1260 Infinity II, Agilent, USA) was equipped with a ZORBAX Extend–C18 column (2.1 mm × 150 mm, 1.8  $\mu$ m) and acetonitrile (solvent A) and 0.1% formic acid in water (solvent B) were used as the mobile phase eluents. The injection volume was 5  $\mu$ L, and the column temperature was set to 30 °C. The total flow rate of the mobile phase was maintained at 0.2 mL/min. The eluent gradient time profile used as follows : (total 15 minutes) 5% A and 95% B at t = 0 min, Then, B was decreased to 5% A from 0 min to 2 min, held at 5% for 2 min, increased to 95% B from 4 min to 5 min, and re–equilibrated from 5 min to 15 min. Full scan monitoring of electrospray ionization MS in the positive/negative mode was used to identify new products in the reaction mixture, and selective ion monitoring to analyze the concentration of N–BOC–His and mono–/di–iodinated N–BOC–Histidine. The following MS settings were used: drying gas (i.e., N<sub>2</sub>) flow rate of 12.0 L/min, nebulizer pressure of 50 psi, drying gas temperature of 350 °C, capillary voltage of 4000 V (positive) and 3500 V (negative), and fragmentor voltages of 90 V.

A QTOF mass spectrometer with a electrospray ionization (ESI) source was used to determine the accurate masses for the parent and product ions of iodinated byproducts formed. The LC–MS/MS–quadrupole time–of–flight (QTOF) analysis was performed using a high–pressure LC instrument (Ultimate3000, Thermo Scientific, USA) coupled to a TripleTOF 5600+ system (AB Sciex, USA) with

a Waters BEH C18 column (2.1 mm  $\times$  100 mm, 1.7  $\mu$ m). For the mobile phase, the eluents were prepared from a mixture of 0.1% formic acid in 10 mM ammonium acetate (solvent C) and methanol (solvent D) at a flow rate of 0.35 mL/min and column temperature of 45 °C. The eluent gradient time profile used for the analysis was as follows: 95% C at  $t = 0$  min, decreased to 70% C from 0.1 min to 8 min, re-declined to 5% C from 8 min to 13 min, held at 5% C from 13 min to 16 min, increased to 95% C from 16.1 min to 20 min. The source conditions of the Triple TOF MS were as follows: nebulizing gas of 50 psi, heating gas of 50 psi, curtain gas of 25 psi, source temperature of 500 °C, declustering potential of  $\pm 60$  V, collision energy of  $\pm 10$  V, and ion spray voltage floating of 5.5 kV. The mass spectra were obtained via full scan and information dependent acquisition scanning in the scan range 30–1000  $m/z$  for MS and MS/MS in both of positive and negative mode. The collision energy spread was  $\pm(35\pm 15)$  eV.

### 2.3.2. GC–MS Analysis

Trihalomethanes and haloacetic acids formed from the chlorination of histidine were determined by an Agilent 7890B gas chromatograph (GC) linked to an Agilent 5977B mass selective detector (MSD). The column used was an HP–5MS 5% phenyl methyl silox (30 m  $\times$  250  $\mu$ m  $\times$  0.25  $\mu$ m). The oven temperature was programmed as follows: an initial temperature of 50  $^{\circ}$ C was held for 5 min, and then increased at a rate of 10  $^{\circ}$ C/min to 160  $^{\circ}$ C; a postrun temperature of 250  $^{\circ}$ C was held for 3 min. Helium was used as the carrier gas and the flow rate was 0.8 mL/min. The inlet temperature was 250  $^{\circ}$ C. The MSD was operated in the electron impact (EI) mode. Selected ion monitoring (SIM) mode was employed for quantification of the THMs and HAAs, and details were described in Table 2.

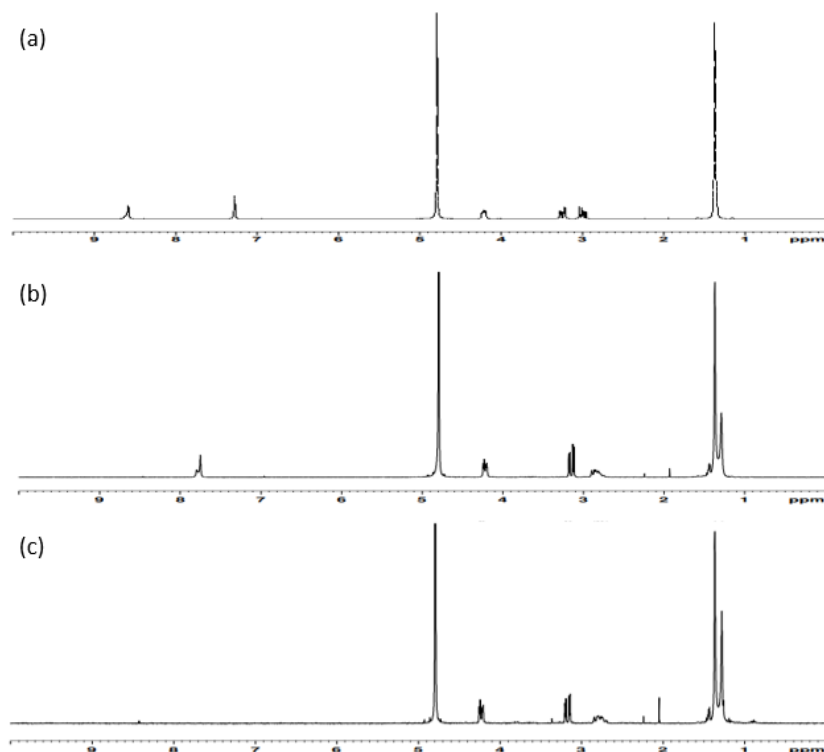
Class	Name	Abbrev.	RT (min)	Selected ion (m/z)
THMs	Trichloromethane	CF	2.28	83
	Dichloriodomethane	DCIM	5.61	85
	Chlorodiiodomethane	DICM	10.76	175
	Triiodomethane	IF	14.59	267
HAAs	Monochloroacetic acid	MCAA	3.95	49
	Dichloroacetic acid	DCAA	6.09	59
	Trichloroacetic acid	TCAA	8.21	119
	Chloriodoacetic acid	CIAA	10.74	175
	Iodoacetic acid	MIAA	8.15	200
	Diiodoacetic acid	DIAA	14.04	127

▲ **Table 2.** THMs and HAAs method information for retention time (min) and selected ion (m/z).

### 2.3.3. $^1\text{H}$ -NMR Analysis and Results

To identify the structures of the synthesized mono- or di-iodinated N-BOC-L-histidine,  $^1\text{H}$ -NMR analysis was further performed. NMR spectra were recorded on a 300 MHz AVANCE III HD (Bruker, German) spectrometer equipped with a  $^1\text{H}$  5-mm probe and used with TopSpin 3.X software. Each NMR samples were prepared by dissolving 5 mg of each final product in 0.5 mL of  $\text{D}_2\text{O}$  solvent. The temperature of the samples was controlled at 298 K during measurement. Sixteen scans were acquired with a spectral width of 6009.615 Hz, an acquisition time of 5.45 sec and a recycle delay of 2 s.

The  $^1\text{H}$  NMR spectra of N-BOC-L-histidine and mono-/di-iodinated N-BOC-L-histidine are shown in Figure 6.



▲ **Figure 7.**  $^1\text{H}$  NMR spectra of (a) N-BOC-L-histidine (b) N-BOC-5-iodo-histidine (c) N-BOC-2,5-iodo-histidine in  $\text{D}_2\text{O}$ . Solvent peak of  $\text{D}_2\text{O}$  at 5.85 ppm.

**N-BOC-L-histidine.**  $^1\text{H}$  NMR (300 MHz,  $\text{D}_2\text{O}$ )  $\delta$  8.59 (s, 1H), 7.28 (s, 1H), 4.21 (q,  $J$  = 4.5 Hz, 1H), 3.24 (q,  $J$  = 6.6 Hz, 1H), 3.00 (q,  $J$  = 8.1 Hz, 1H), 1.37 (s, 1H).

**N-BOC-5-iodo-L-histidine.**  $^1\text{H}$  NMR (300 MHz,  $\text{D}_2\text{O}$ )  $\delta$  7.77 (d,  $J$  = 13.6 Hz, 1H), 4.21 (q,  $J$  = 4.6 Hz, 1H), 3.14 (q,  $J$  = 6.4 Hz, 1H), 2.85 (q,  $J$  = 8.0 Hz, 1H), 1.36 (s, 1H), 1.28 (s, 1H).

**N-BOC-2,5-iodo-L-histidine.**  $^1\text{H}$  NMR (300 MHz,  $\text{D}_2\text{O}$ )  $\delta$  4.23 (q,  $J$  = 4.8 Hz, 1H), 3.17 (q,  $J$  = 6.3 Hz, 1H), 2.77 (m,  $J$  = 9.0 Hz, 1H), 1.36 (s, 1H), 1.28 (s, 1H).

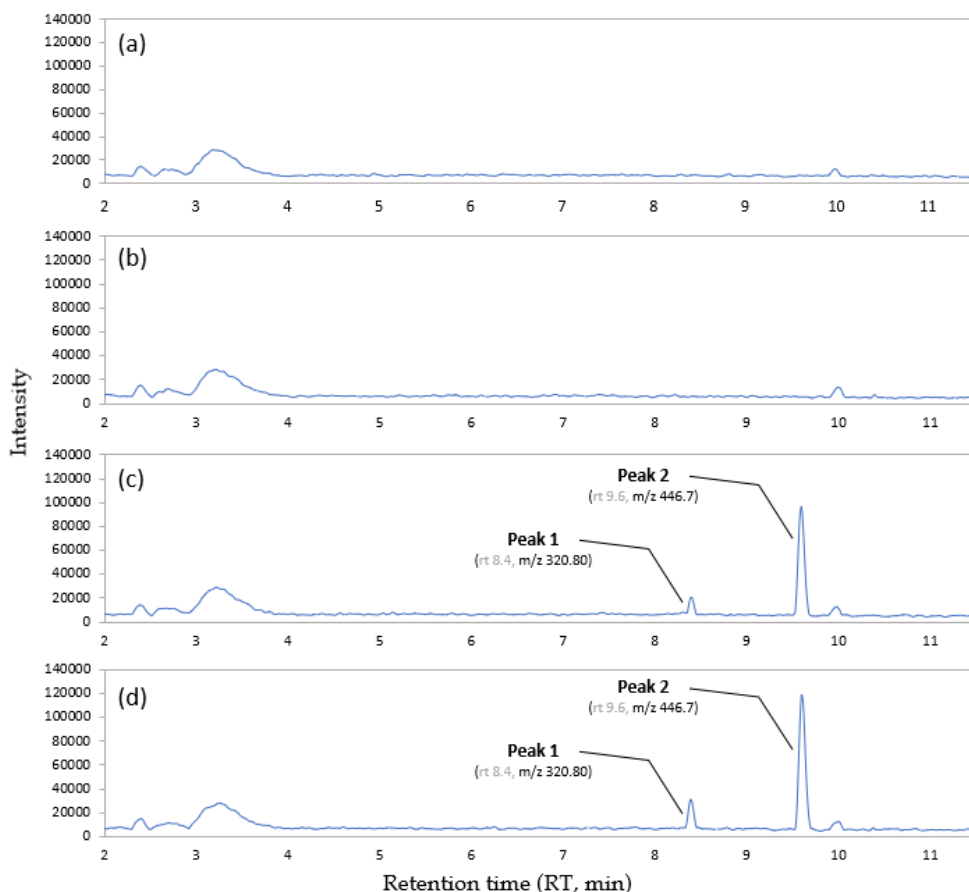
## Chapter 3. Results and Discussion

### 3.1. Identification of Iodinated Byproducts from Imidazole Compounds during Chlorination with Iodide-Containing Water

In order to identify iodinated DBPs formed from compounds that have imidazole moieties, each chlorination experiment of imidazole-carboxylic, phenyl-imidazole-carboxylic acid, and histidine was conducted. After 24 h chlorination in the presence of iodide, we obtained full scan ( $m/z$  100–600) mass spectra of each chlorinated water sample.

#### 3.1.1. Imidazole-Carboxylic Acid

For controlled samples, the reaction of imidazole-carboxylic acid with iodide but without chlorination resulted in no formation of iodinated products. Of course, for the chlorination of imidazole-carboxylic acid without iodide, no iodinated products were formed. It was evident that the iodinated histidine products are produced only from chlorination in the presence of iodide.



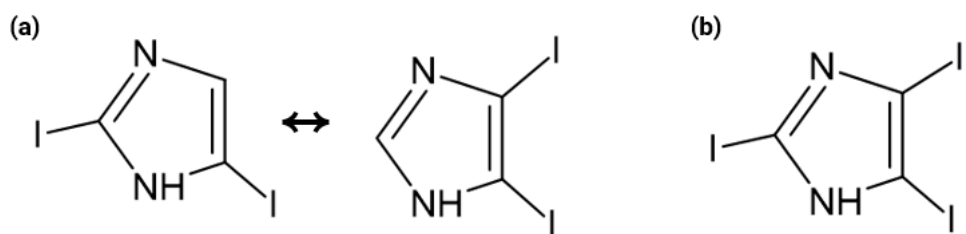
▲ **Figure 8.** LC/(+)ESI-MS TIC chromatograms after chlorination of the imidazole-carboxylic acid in the presence of 50  $\mu\text{M}$  of imidazole-carboxylic acid with (a) no oxidants (b) only 100  $\mu\text{M}$   $\text{Cl}^-$  (c) 100  $\mu\text{M}$   $\text{Cl}^-$  and 50  $\mu\text{M}$   $\text{I}^-$  (d) 100  $\mu\text{M}$   $\text{Cl}^-$  and 100  $\mu\text{M}$   $\text{I}^-$ .

Figure 7a–d. show LC–MS mass spectra using positive full scan mode after 24h chlorination of the imidazole-carboxylic acid (Imi-COOH). There were no new peaks formed in the control (Figure 7a) and in the only chlorine reaction (Figure 7b). However, under the chlorination in the presence of iodide, a distinct decrease in Imi-COOH was observed and two peaks were newly formed, as shown in Figure 7c–d. The new peak 1 which of the  $[\text{M}+\text{H}]^+$  ion is  $m/z$  320.8 differs 208 Da from the  $m/z$  of Imi-COOH. The observed mass difference corresponded to the substitution of two proton ( $-2\text{H}$ ,  $-2$ ) by two iodine atom ( $+2\text{I}$ ,  $+254$ ) after the decarboxylation

( $-\text{COO}$ ,  $-44$ ). In addition, peak 2 showed an  $m/z$  446.7 of  $[\text{M}+\text{H}]^+$  ion, indicating one more iodine substitution ( $-^1\text{H}$ ,  $+^{127}\text{I}$ ) has occurred from the compound of peak 1. Thus, these final products were matched with di-I-imidazole and tri-I-imidazole.

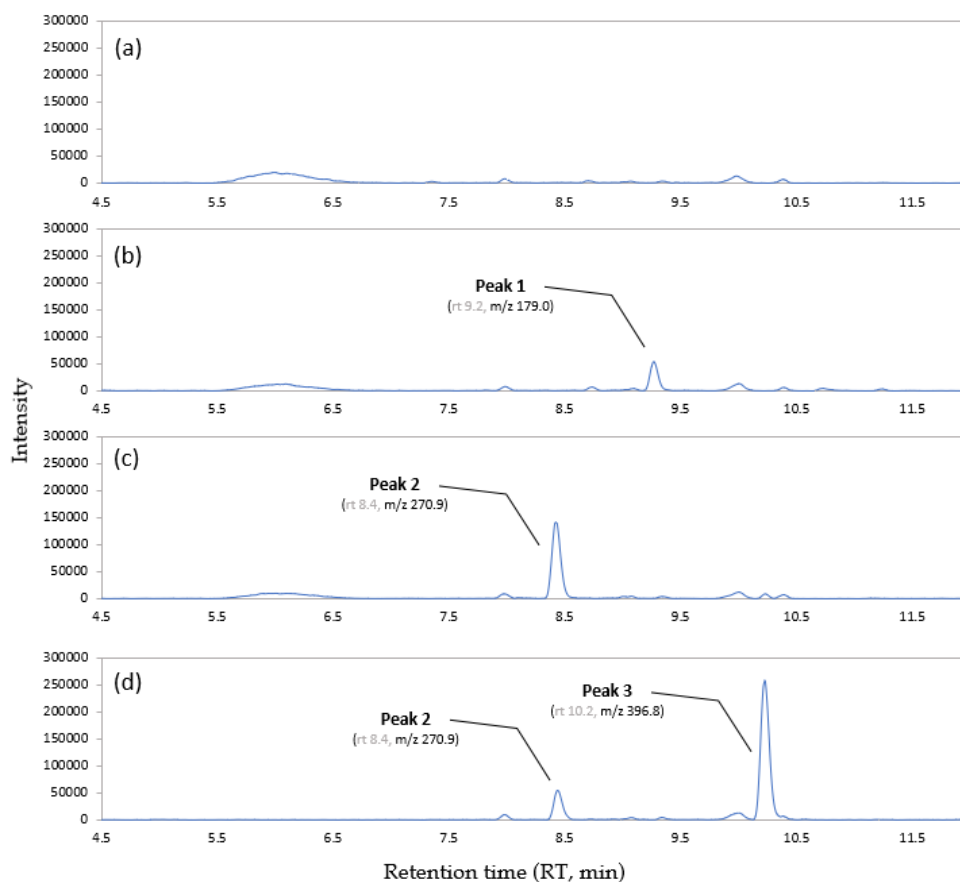
During the chlorination, imidazole-carboxylic acid initially undergoes decarboxylation. This hypothesis is consistent with other mechanisms that free amino acids eliminate the carboxyl group to generate more simple compounds.<sup>23</sup> There are two main steps in the electrophilic reaction process. First, electrophile  $\text{I}^+$  (from  $\text{HOI}$ ), which acts as a acid, attacks the imidazole ring ( $\text{pK}_a$  7.0) forming  $\pi$ -complexes on the nitrogen ( $\text{N3}$ ), and then induces the hydrogen atom connected to the nitrogen ( $\text{N1}$ ) leaving away. The reason is that the HDE of the  $\text{H}-\text{N1}$  bond is dramatically lower than that of other bonds. Thus, the H atom connected to  $\text{N1}$  is much easier to release in the proton form than other H atoms.<sup>24</sup> Second, the electrophile  $\text{I}^+$  on the nitrogen ( $\text{N3}$ ) transfers to one of carbon atom of imidazole ring ( $\text{C2}/\text{C4}/\text{C5}$ ) to change to  $\sigma$ -complexes. It is explained by relative energy (RE) for the end halogenated products at each site of imidazole ring. *Han et al., (2020)* reported that RE of the chlorinated end products at the C2, C4, and C5 sites had negative values relative to that at the N3, and suggested the thermodynamic reactivity order of  $\text{C4} \approx \text{C5} > \text{C2} \gg \text{N3}$ .<sup>37</sup> This implies that the same mechanism can be applied to  $\text{I}^+$  other than  $\text{Cl}^+$ . In conclusion, the kinetically rapidly formed 3-I-Imi may be converted into the thermodynamically more stable product 2/4/5-I-Imi. Therefore, the final iodinated imidazole is a form in which iodine is substituted on a carbon atom. Moreover, imidazole-carboxylic acid showed that it can further react with electrophiles to produce di-iodinated and tri-iodinated byproducts from the chlorination of iodide-containing water.





▲ **Figure 9.** Proposed structures of (a) di-I-imidazole (b) tri-I-imidazole.

### 3.1.2. Phenyl–Imidazole–Carboxylic Acid

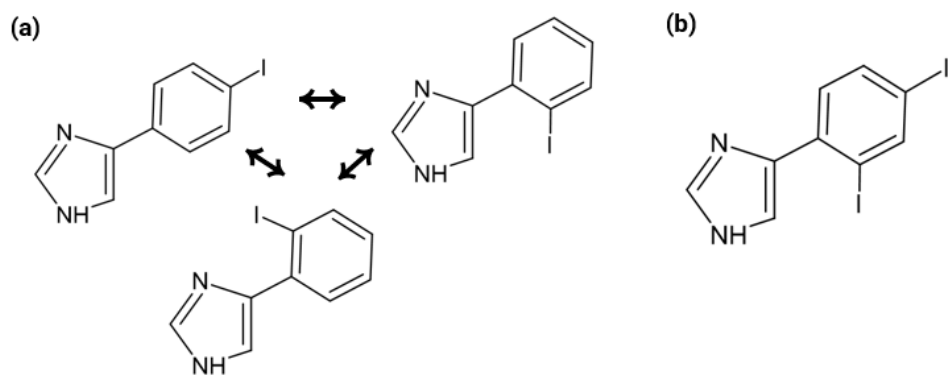


▲ **Figure 10.** LC/(+)ESI-MS TIC chromatograms after chlorination of the phenyl–imidazole–carboxylic acid in the presence of 50  $\mu\text{M}$  of phenyl–imidazole–carboxylic acid with (a) no oxidants (b) only 100  $\mu\text{M}$  Cl<sup>-</sup> (c) 100  $\mu\text{M}$  Cl<sup>-</sup> and 50  $\mu\text{M}$  I<sup>-</sup> (d) 100  $\mu\text{M}$  Cl<sup>-</sup> and 100  $\mu\text{M}$  I<sup>-</sup>

Figure 9a–d. show LC–MS mass spectra using positive full scan mode after 24h chlorination of the phenyl–imidazole–carboxylic acid (Phe–Imi–COOH). Compared with the blank, one peak was detected in the TIC of the chlorinated histidine solution without iodine or with iodine, and two peaks were detected in the solution with high iodine concentration. In particular, unlike Imi–COOH, mono–chlorinated and mono–iodinated derivatives were observed in the Phe–Imi–COOH samples. The peak 1, as shown in Figure 9b, showing m/z of 179.0, corresponded to the protonated molecular ion

( $[M+H]^+$ ) of chlorinated phenyl-imidazole. It is inferred that this compound was formed through decarboxylation ( $-COO$ ,  $-44$ ) and a chlorine substitution ( $-^1H$ ,  $+^{35}Cl$ ) through the mechanism presented above 3.1.1.. In the iodide-containing chlorination, new peaks 2 and 3 were the  $[M+H]^+$  ion  $m/z$  270.9 and 396.8, representing that the mono-iodinated ( $-^1H$ ,  $+^{127}I$ ) and di-iodinated ( $-2\ ^1H$ ,  $+2\ ^{127}I$ ) Phe-Imi after decarboxylation ( $-COO$ ,  $-44$ ). Moreover, as the iodide concentration increased (Figure 9c-d), it was observed that the intensity of mono-iodinated Phe-Imi decreased and that of di-iodinated Phe-Imi increased. It means that an additional iodine substitution was occurred from mono-iodo to di-iodo.

Unfortunately, the exact molecular structure of iodinated Phe-Imi could not be confirmed because LC-MS/MS analysis was not performed. But based on the previous papers, iodine substitution sites were inferred. Phenyl-imidazole-carboxylic acid is a polycyclic aromatic compound containing a benzene ring linked to an imidazole ring through a C-C bond. Generally, a benzene ring is susceptible to electrophilic attack and contains two activating halogen substitutions in *ortho* and *para* positions.<sup>31</sup> Halogenation takes place preferentially in benzene ring than in imidazole ring because the resonance hybrid structure of benzene has an abundance of electrons and is more stable. Hence, in the compound in which imidazole coexists with phenyl, like phenyl-imidazole carboxylic acid, the imidazole group cannot provide an iodine substitution site because of a relatively low electron-donating potential than the phenyl group.

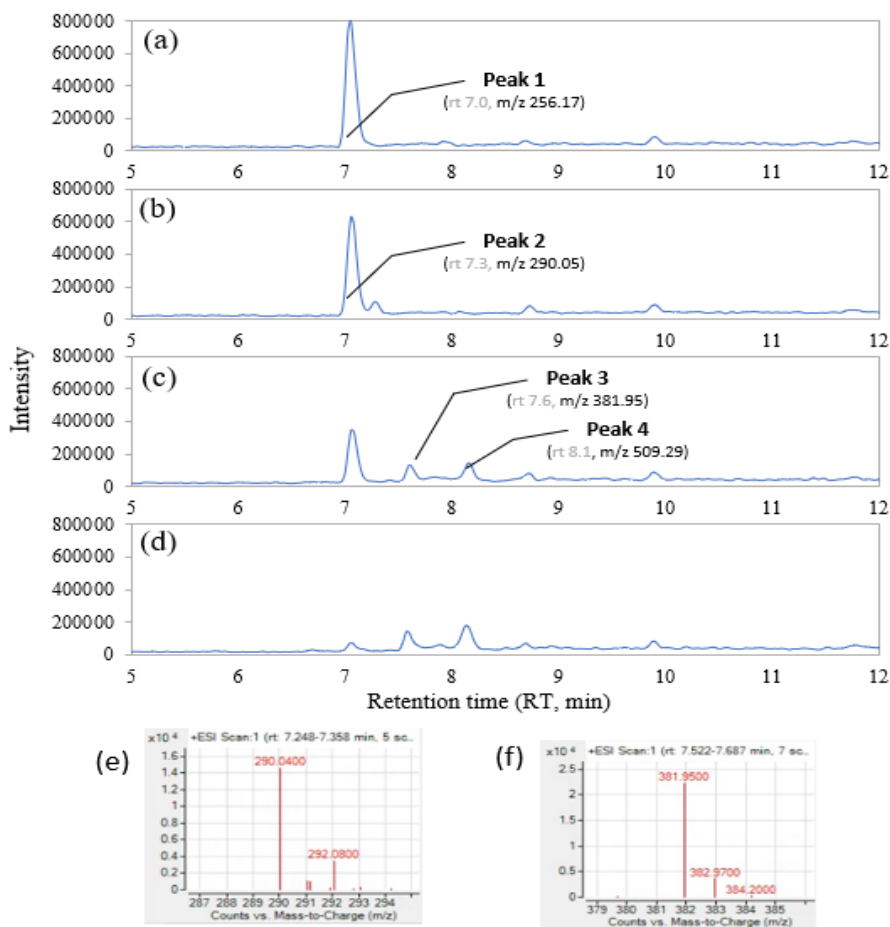


▲ **Figure 11.** Proposed structures of (a) I-phenyl-imidazole (b) di-I-phenyl-imidazole.

### 3.1.3. Histidine

Amino acids have the largest proportion of dissolved organic nitrogen (DON), and most exist in peptides or proteinous forms. Histidine is one of essential amino acids and has two possible sites for iodine substitution: the  $\alpha$ -amino group and the imidazole ring side chain. In this study, we used N-tert-Butyloxycarbonyl histidine (N-BOC-His) to mimic peptide bonds, to prevent the iodination of  $\alpha$ -amino group, and only to see the reactivity of the imidazole ring with HOI. When the amine group bonds with the BOC group, an amide group is formed, causing the delocalization of the lone pair of amide nitrogen to carbonyl oxygen. Since the electron density of amide is lowered, making it less basic than the original amine, it indicates that the amide linkage does not participate significantly in electrophilic substitution. Thus, we expected that the halogen substitution reaction would occur in the imidazole ring, not the  $\alpha$ -amino group.<sup>25</sup> The hypothesis can also be explained by the relatively slow reaction of amide nitrogen with HOCl.<sup>26</sup>

In the controlled water samples, chlorination of histidine without iodide resulted in no formation of iodinated products, but chlorinated histidine derivatives were observed. It indicates that chlorine substitution in imidazole is the predominant reaction during chlorination in the absence of iodide. Thus, we identified chlorinated or iodinated histidine products by LC-MS and MS/MS analysis of chlorinated water.

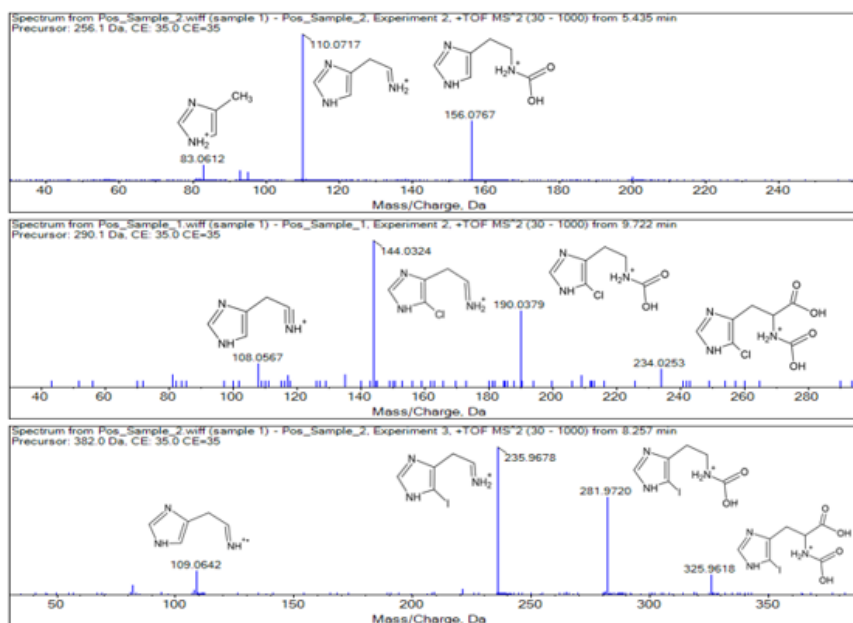


▲ **Figure 12.** LC/(+)ESI-MS TIC chromatograms after chlorination of the histidine in the presence of 5  $\mu$ M of N-BOC-His with (a) no oxidants (b) only 10  $\mu$ M  $\text{Cl}^-$  (c) 10  $\mu$ M  $\text{Cl}^-$  and 5  $\mu$ M  $\text{I}^-$  (d) 10  $\mu$ M  $\text{Cl}^-$  and 10  $\mu$ M  $\text{I}^-$ . (e–f) mass spectra of peak 2 and peak3, showing isotope patterns of chlorinated N-BOC-His and iodinated N-BOC-His.

Figure 11a–d show LC–MS mass spectra using positive full scan mode after 24h chlorination of the histidine in the presence of 5  $\mu$ M of histidine with (a) no oxidants (b) only 10  $\mu$ M  $\text{Cl}^-$  (c) 10  $\mu$ M  $\text{Cl}^-$  and 5  $\mu$ M  $\text{I}^-$  (d) 10  $\mu$ M  $\text{Cl}^-$  and 10  $\mu$ M  $\text{I}^-$ . Compared to the blank, three main peaks were detected in the TIC of chlorinated histidine solutions with and without iodide. Since peak 1 had the same retention time and mass spectrum as the histidine standard, peak 1 ( $[\text{M}+\text{H}]^+$  ion at  $m/z$  256.17) was identified as unreacted histidine remaining after chlorination. The new peak 2 which of the

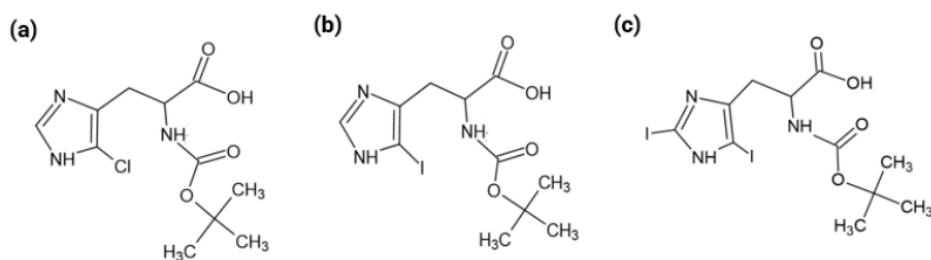
$[M+H]^+$  ion was  $m/z$  290.05 differs 34 Da from the  $m/z$  of N-BOC-His. The observed mass difference corresponded to the substitution of one proton ( $-1$ ) by one chlorine atom ( $+35$  or  $+37$ ). It represents the formation of the protonated molecular ion of chlorinated N-BOC-His. Similarly, the other new peak 3, showing a mass difference of 126 Da from the  $m/z$  of N-BOC-His, is consistent with the iodinated N-BOC-His resulted from the substitution of one proton ( $-1$ ) with one iodine atom ( $+126.9$ ).

Furthermore, the isotopic pattern of the mass spectra agreed with the theoretical pattern of a compound containing one chlorine atom. Based on the natural  $^{35}\text{Cl}/^{37}\text{Cl}$  abundance of 3/1, the ratio of the peak intensity of  $M/M+2$  (containing  $^{35}\text{Cl}/^{37}\text{Cl}$ ) should also be 3/1. In the mass spectra of the chlorinated N-BOC-His, a pair of peaks with 290 and 292 was appeared, and the ratio of the peak abundances was 3/1, as shown in Figure 11e. Unlike chlorinated histidine, iodinated N-BOC-His (Figure 11f) showed no isotope as containing only  $^{127}\text{I}$  atoms.



▲ **Figure 13.** LC-QTOF-MS/MS mass spectra of (a)  $m/z$  256.1291, (b)  $m/z$  290.0896, (c)  $m/z$  382.0255.

To match their accurate masses with the molecular formulas and to identify the structures of the chlorinated and iodinated products formed, we further performed MS/MS analysis and acquired the fragments of these products. Figure 12a–c show LC–QTOF–MS/MS spectra of N–BOC–His, N–BOC–Cl–His, and N–BOC–I–His. For an example of iodinated N–BOC–His (Figure 12c), the protonated molecular ion ( $[M+H]^+$ ) was  $m/z$  382.0255 with a mass accuracy of 0.1 ppm. Their characteristic fragments at  $m/z$  325.9618, 281.9720, 235.9678, and 109.0642 show one iodine atom substitution on the imidazole group of histidine. Similarly, Figure 12b shows the fragment ions of chlorinated (containing  $^{35}\text{Cl}$ ) N–BOC–His  $m/z$  290.0896 with mass accuracy of 0.3 ppm, including  $m/z$  234.0253, 190.0379, 144.0324, and 108.0567. Although not shown here, N–BOC–di–I–His ( $[M-H]^-$   $m/z$  505.9106,  $\Delta m$  –0.1 ppm) were also detected in the negative full scan mode. As a result, the characteristic fragment demonstrated the substitution of chlorine and iodine atoms in the imidazole group by proposing the structure of the compound, as shown in Figure 13.



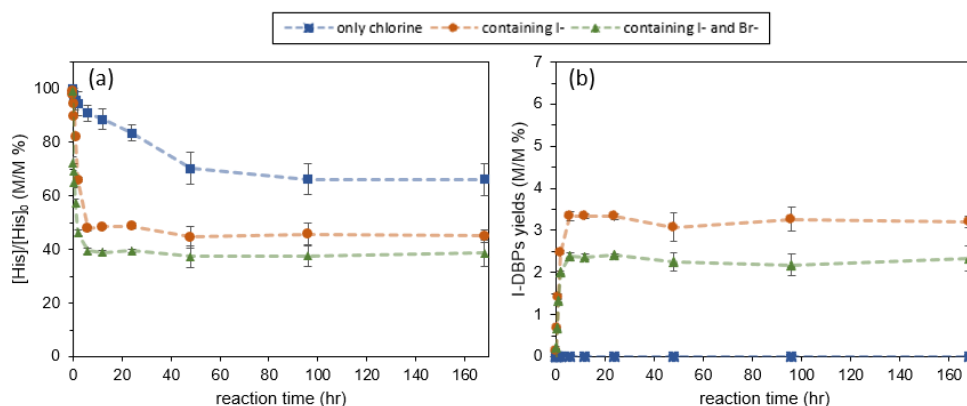
▲ **Figure 14.** Proposed structures of (a) N–BOC–Cl–histidine (b) N–BOC–I–histidine (c) N–BOC–di–I–histidine.

We will focus on histidine reactivity and the formation of iodinated products in the next chapters.



### 3.2. Kinetics Study of Histidine Reactivity and Iodinated Byproducts Formation

The degradation of N-BOC-His (initial 5  $\mu$ M) and the formation of iodinated histidine products were determined as a function of time for the three chlorination conditions at pH 7 for 7-days: only chlorination (HOCl 10  $\mu$ M), containing iodide (KI 5  $\mu$ M), and containing iodide and bromide (KI 5  $\mu$ M and NaBr 50  $\mu$ M).



▲ **Figure 15.** (a) The degradation of histidine and (b) the formation of iodinated histidine products as a function of reaction time (hr). Experimental conditions:  $[\text{N-BOC-His}]_0 = 5 \mu\text{M}$ ,  $[\text{NaOCl}]_0 = 10 \mu\text{M}$ ,  $[\text{I}^-]_0 = 0$  or  $5 \mu\text{M}$ ,  $[\text{Br}^-]_0 = 0$  or  $50 \mu\text{M}$ , phosphate buffer, pH 7.0, reaction time = 0–7 days.

Compared to a reaction without iodide and bromide, the loss kinetics of histidine in chlorinated solutions containing 5  $\mu$ M of  $\text{I}^-$  or 5  $\mu$ M of  $\text{I}^-$  and 50  $\mu$ M of  $\text{Br}^-$  were accelerated, as shown in Figure 14a. In the presence of iodide and bromide, HOI and HOBr are formed immediately after free chlorine addition with rate constants of  $4.3 \times 10^8 \text{ M}^{-1}\text{s}^{-1}$  and  $1.6\text{--}6.8 \times 10^3 \text{ M}^{-1}\text{s}^{-1}$ , respectively.<sup>27,28,29</sup> Moreover, natural organic matter reacts faster in order of HOI, HOBr, and HOCl.<sup>30,31</sup> Thus, it is important to note that the observed difference in chlorination kinetics is due to the overall reaction rate according to the types and amounts of various active oxidizing agents induced by the iodide and bromide.

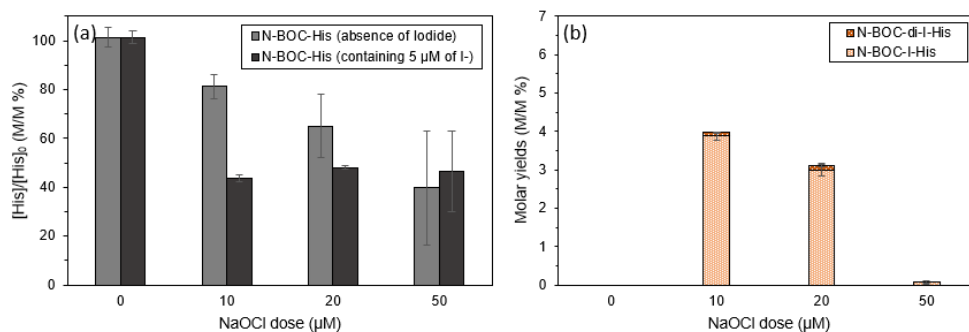
In this study, for the only chlorine condition, the total histidine residue declined over a 4-days and finally had minimum of 65.33 %. However, in the iodide-containing conditions, the reaction was determined within 6 hours, and the minimum histidine residue was 45.32 %. In the coexist of bromide condition, the rate-determining reaction occurred within 6 hours, similar to the iodide condition, but the remaining concentration of histidine was lower, which accounted for 37.35 %, than iodide-containing condition. Since the rate constant of HOBr is about three to four orders of magnitude higher than for HOCl,<sup>32</sup> the remaining HOCl was converted to a more reactive HOBr under the bromide-containing system, causing a slightly higher loss of histidine.

Figure 14b. shows the cumulative yields of N-BOC-I-His and N-BOC-di-I-His. In the iodide-containing condition, the maximum molar yield of 3.33 % was achieved within 6 hours, as well as in the coexist of bromide, the maximum yield of 2.40 % appeared at 6 hours. The yield of iodinated histidine products in the bromide-containing condition decreased slightly due to the increase in the overall strength of the mixed oxidants caused by the proportions of HOI, HOBr, and HOCl. Nevertheless, there was no change in the molar yield during the 7-day period under both conditions. It indicates that the iodinated histidine products are stable in the chlorinated water and have potential existence in the real chlorinated water.

### 3.3. Factors Influencing Histidine Degradation and Iodinated Histidine Products Formation

In the reaction process with iodide, the degradation of histidine and the formation of iodinated histidine products were stable at 24 h. Therefore, in the following experiment, the sampling end point was selected as 24 hours.

#### 3.3.1. Chlorine Dose

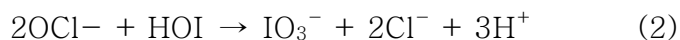
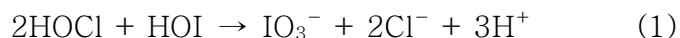


▲ **Figure 16.** Effect of initial NaOCl dose on (a) the degradation of histidine and (b) the formation of iodinated histidine products in the presence of iodide 5  $\mu M$ . Experimental conditions:  $[N-BOC-His]_0 = 5 \mu M$ ,  $[NaOCl]_0 = 0-50 \mu M$ ,  $[I^-]_0 = 0$  or  $5 \mu M$ , phosphate buffer, pH 7.0, reaction time = 24 h.

Figure 15. shows the effect of NaOCl dose on the degradation of histidine and the formation of iodinated histidine products. As a results, the degradation rate of histidine increased with an enlarging of the NaOCl dose. In particular, as shown in Figure 15a, when iodide was present, the overall reaction rate was increased (discussed in 3.2.), so the decomposition rate of histidine was remarkably increased. At low NaOCl concentration of 10  $\mu M$ , the remaining histidine after 24 hours of reaction in the absence of  $I^-$  was 81.27 %, whereas, in the presence of 5  $\mu M$  of  $I^-$ , the amount

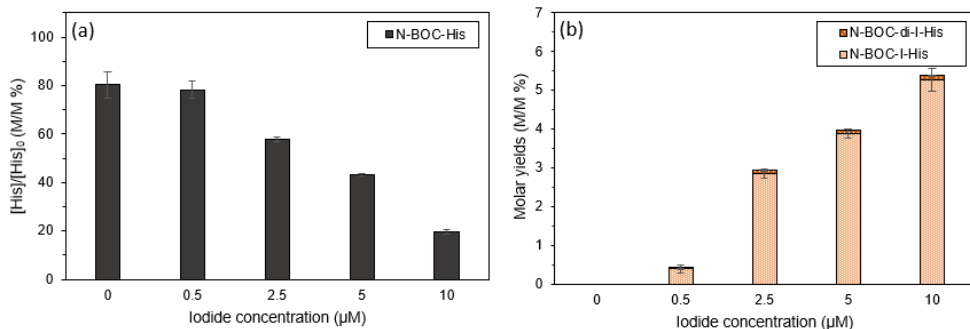
of histidine decreased sharply to 43.77 %.

However, for the formation of iodinated histidine products (Figure 15b), the maximum cumulative molar yield, which accounted for 3.97 %, decreased to 0.07 % when increasing the NaOCl dose from 10  $\mu$ M to 50  $\mu$ M. Because HOCl is present in excess relative to HOI, the further oxidation step from HOI to  $\text{IO}_3^-$ , which is an unreactive iodine species, occurs according to reaction (1) and (2).<sup>10</sup>



Moreover, high NaOCl concentration increases the competitive opportunity for HOCl to attack the reactive site of histidine where iodine substitution occurs by HOI. Therefore, this limitation on the iodine substitution reaction of histidine considerably reduces the possibility of the formation of iodinated histidine products.

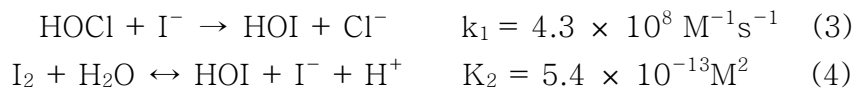
### 3.3.2. Iodide Concentration



▲ **Figure 17.** Effect of  $\text{I}^-$  concentration on (a) the degradation of histidine and (b) the formation of iodinated histidine products. Experimental conditions:  $[\text{N-BOC-His}]_0 = 5 \mu\text{M}$ ,  $[\text{NaOCl}]_0 = 10 \mu\text{M}$ ,  $[\text{I}^-]_0 = 0 - 10 \mu\text{M}$ , phosphate buffer, pH 7.0, reaction time = 24 h.

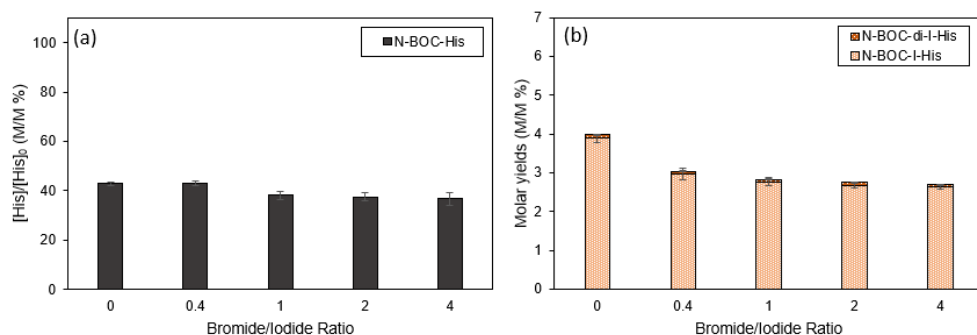
As shown in Figure 16, with the increase in iodide concentration from 0  $\mu\text{M}$  to 10  $\mu\text{M}$ , the concentration of remaining histidine decreased, but the yield of iodinated histidine products increased. The amount of histidine remaining after chlorination at 0  $\mu\text{M}$   $\text{I}^-$  was 80.32% relative to the initial histidine, and histidine decreased to 19.53% as the iodide concentration increased to 10  $\mu\text{M}$ . In addition, although the HOI concentration was twice that of histidine (at 10  $\mu\text{M}$   $\text{I}^-$ ), it was confirmed that histidine degradation occurred 2.5 times more in NaOCl 50  $\mu\text{M}$ , which is a 10-fold concentration of histidine (Figure 16a).

Accordingly, the yield of iodinated histidine products increased gradually up to 5.37 % at 10  $\mu\text{M}$  of  $\text{I}^-$ , meaning that the tendency for histidine to be converted to the iodinated form is increased. The result could be explained by the disproportionation of  $\text{I}^-$ . The reaction with an excess of  $\text{I}^-$  leads to the formation of more HOI and  $\text{I}_2$ , as described by reactions (3) and (4).



The reactive iodine species (HOI and I<sub>2</sub>) might react with NOM, such as histidine here. Thus, increased formation of available reactive iodine species may induce the increasing chance of iodine substitution of histidine, resulting in more production of iodinated histidine products. However, the formation of N-BOC-di-I-His was still 0.03 %, and it did not show a significant value except that histidine could be iodinated from mono-I- to di-I-.

### 3.3.3. Bromide/Iodide Molar Ratio



▲ **Figure 18.** Effect of  $\text{Br}^-/\text{I}^-$  molar ratio on (a) the degradation of histidine and (b) the formation of iodinated histidine products. Experimental conditions:  $[\text{N-BOC-His}]_0 = 5 \mu\text{M}$ ,  $[\text{NaOCl}]_0 = 10 \mu\text{M}$ ,  $[\text{I}^-]_0 = 5 \mu\text{M}$ ,  $[\text{Br}^-]_0 = 0\text{--}20 \mu\text{M}$  phosphate buffer, pH 7.0, reaction time = 24 h.

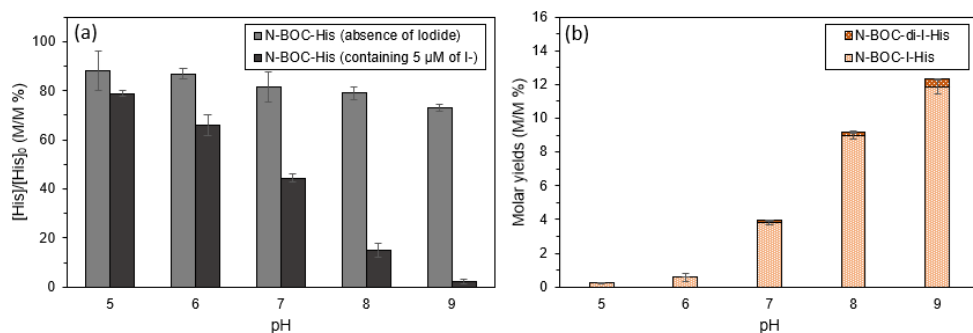
$\text{Br}^-$  and  $\text{I}^-$  are often introduced into source water, and the molar ratio of  $\text{Br}^-/\text{I}^-$  varies. *Richardson et al.*, (2008) reported concentrations of  $\text{Br}^-$  ( $24\text{--}1120 \mu\text{g L}^{-1}$ ) and  $\text{I}^-$  ( $0.4\text{--}104 \mu\text{g L}^{-1}$ ) and  $\text{Br}^-/\text{I}^-$  molar ratios ranging from 0.24 to 21.6 in the source of drinking water treatment plant (DWTPs in 22 cities of USA and 1 of Canada).<sup>33</sup>  $\text{Br}^-$  also can be easily oxidized to  $\text{HOBr}$  by  $\text{HOCl}$ , like  $\text{HOI}$ , and their combined effect can affect the formation of halogenated disinfection byproducts during chlorination.

Figure 17. shows the effect of  $\text{Br}^-/\text{I}^-$  molar ratio during chlorination of histidine. The concentration range of injected  $\text{Br}^-$  was  $0\text{--}20 \mu\text{M}$  in the presence of  $5 \mu\text{M I}^-$ . As shown in Figure 17a, despite the increase in the  $\text{Br}^-/\text{I}^-$  ratio, the remaining histidine residues were constant in the range of 37–43 %. For the production of iodinated histidine products, the yields slightly decreased from 3.97 % to 2.69 % when bromide was present. The increase in  $\text{Br}^-/\text{I}^-$  ratio means an increase in  $\text{HOBr}$  production, which leads to produce relatively less  $\text{HOI}$ , resulting in fewer iodinated byproducts. Moreover,  $\text{HOBr}$ , formed through reaction, could induce the

formation of brominated byproducts. However, since the reactivity of HOI to NOM is higher than that of HOBr, HOI favors halogen substitution and preferentially causes the formation of iodinated byproducts. Hence, there was no significant effect on the yield change of the iodinated histidine products according to the concentration of bromide.



### 3.3.4. pH of Solution



▲ **Figure 19.** Effect of pH on (a) the degradation of histidine and (b) the formation of iodinated histidine products in the presence of iodide 5  $\mu$ M. Experimental conditions:  $[N\text{-BOC-His}]_0 = 5 \mu\text{M}$ ,  $[\text{NaOCl}]_0 = 10 \mu\text{M}$ ,  $[I^-]_0 = 0\text{--}5 \mu\text{M}$ , phosphate buffer, pH 5–9, reaction time = 24 h.

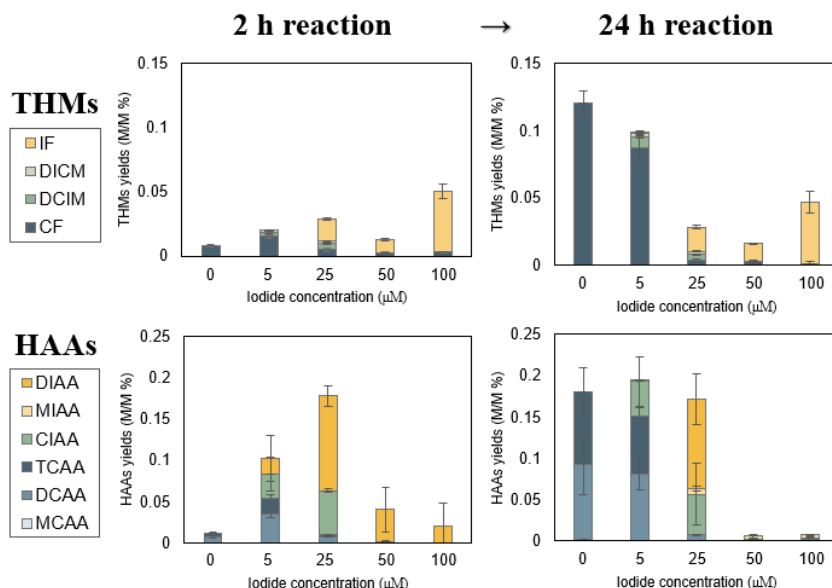
As shown in Figure 18, solution pH significantly affected the degradation of histidine and the formation of iodinated histidine products when chlorination occurred with iodide-containing water. The residual concentration of histidine showed a slight decrease of 15.04 % (88.07 %  $\rightarrow$  73.04 %) in the chlorination without iodide as pH increased from 5 to 9. Conversely, it showed a dramatic decrease of 76.67% (78.87 %  $\rightarrow$  2.20 %) in the iodide-containing condition. The concentration of N-BOC-I-His was at a minimum molar yield of 0.26 % relative to the initial histidine at pH 5, but increased to a maximum of 11.85 % at pH 9. Furthermore, N-BOC-di-I-His was not detected at pH 5 and 6, but it exhibited 0.09 % at pH 7, 0.26 % at pH 8, and a maximum of 0.47 % at pH 9. These results suggest that the increase in pH would activate the reactivity of iodine species. It binds to histidine and consequently promotes the formation of iodinated histidine products.

The pH-dependent change can be mainly due to two aspects: First, the disproportion of iodine oxidant species is dependent on pH. Generally, by reaction (4),  $I_2$  is the dominant iodine species at acidic pH (under pH 6.13), whereas HOI becomes predominant at neutral and nearly alkaline conditions. HOI and  $I_2$  have different

reduction potentials depending on the iodine oxidation state when HOI is +1 and  $I_2$  is 0. The standard reduction potential of HOI (+1.45V) is much higher than that of  $I_2$  (+0.62V), suggesting that HOI is a more efficient oxidizing agent for iodine substitution in histidine.<sup>34</sup> Second, pH affects the speciation of histidine. Since the pK value at 25 °C of histidine of the imidazole group is 6.1, as pH increases, the electron neutral molecule of histidine also increases. Moreover, the greater activity behavior of the electrophile HOI shifts to higher pH because of a higher pKa of 10.4. In terms of the mechanism of electrophilic substitution, iodination could be explained by the action of an electrophile (HOI, +1) as an electron-accepting acid that attacks the lone pair of electrons in imidazole, which has base properties. The hydrogen atom linked to the imidazole ring then breaks off to form  $H^+$ , but under acidic conditions it is difficult to release  $H^+$ . Thus, pH affects the equilibrium of the reaction. As a result, the concentration of the histidine iodide product formed was higher at higher pH values due to the simultaneous effect of pH on the activity of histidine and HOI.

### 3.4. Comparison of Yields of Iodinated Histidine Products with Other Regulated DBPs (THMs and HAAs)

We addressed chlorinated or iodinated THMs and HAAs production potentials of histidine and compared the yields with iodinated histidine products formed from chlorinated iodide-containing water. During the last 20 years, many research found that chlorination of dissolved amino acids leads to the formation of toxic disinfection by-products (DBPs) such as trihalomethanes (THMs) and haloacetic acids (HAAs), but with low yields. *Hureiki et al.*, (1944) have reported that most of the free amino acids could be precursors of chloroform, with yields below 1%.<sup>35</sup> *Scully et al.*, (1985) observed that the chloroform yields produced by proteins were low at around 0.5%.<sup>36</sup> The results obtained, in this study, corresponds to the study above in that the maximum total yield of THM and HAA was less than 0.4% in histidine chlorination.

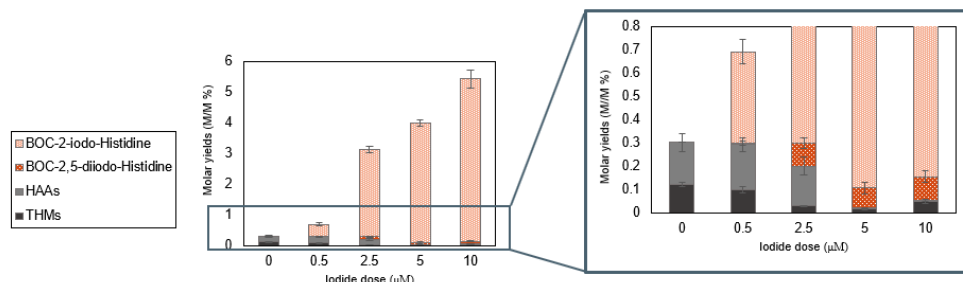


▲ **Figure 20.** Effect of  $\text{I}^-$  concentration and chlorine reaction time on the formation of THMs and HAAs during chlorination of histidine. Experimental conditions:  $[\text{N-BOC-His}]_0 = 50 \mu\text{M}$ ,  $[\text{NaOCl}]_0 = 100 \mu\text{M}$ ,  $[\text{I}^-]_0 = 0 - 100 \mu\text{M}$ , phosphate buffer, pH 7.0, reaction time = 2 h or 24 h.

The species of disinfection byproducts can vary affected by the concentration of halides in source waters, and the DBPs formation also depends on reaction time with chlorine. Figure 19. shows the formation of THMs and HAAs in different concentrations of iodide and reaction time during chlorination of histidine. As shown in Figure 19, as reaction time was longer, from 2 h to 24 h, the formation of DBPs was higher in both of THMs and HAAs. After the chlorination with 0  $\mu\text{M}$  of  $\text{I}^-$  for 24 h, chloroform (CF), dichloroacetic acid (DCAA), and trichloroacetic acid (TCAA) showed the highest molar yields of THMs and HAAs compared to initial molar concentration of N-BOC-His, accounted for 0.121 %, 0.091 %, and 0.088 %, respectively. At this time, the reason for the dramatical increase of total yields of THMs and HAAs at 24 h rather than 2 h is the difference in chlorination rate according to the iodide concentrations. In addition, as chloro-iodo- or iodo-DBPs species were found in the presence of iodide, the yield of chlorinated DBPs was converted to iodinated DBPs in terms of species proportion. The domain species of formed I-THMs was iodoform (IF), which accounted for 0.045 % in chlorinated water containing 100  $\mu\text{M}$   $\text{I}^-$ .

For I-HAAs, diiodoacetic acid (DIAA) was the dominant species and had the highest molar yield of 0.115 % at 25  $\mu\text{M}$  of  $\text{I}^-$ , after two-hour reaction. However, the production of DIAA decreased from 2 h to 24 h due to the stability of DIAA. This result suggests two possibilities. The first possibility is a decomposition of DIAA by the further oxidation of HOI. The second one the transition of DIAA to TIAA. Because increasing reaction time with HOI likely induces one more electrophilic substitution of iodine, it is likely that the final product may be changed from DIAA to TIAA. For example, *Liu. et al., (2017)*<sup>37</sup> reported that TIAA produced five times more than DIAA during chloramination of real waters spiked with iodide. Unfortunately, in this study, triiodoacetic acid (TIAA) could not be quantified because a standard could not be obtained, but, like

trichloroacetic acid (TCAA), we expected further iodination of DIAA may encourage TIAA formation.



▲ **Figure 21.** Comparison of molar yields of iodinated histidine products with THMs and HAAs formed after 24 h chlorination.

Figure 20. shows the formation of iodinated histidine products, THMs, and HAAs formed from the 24 h chlorination of histidine with iodide concentrations in pH 7. As a comparison, we found that N-BOC-I-His was the predominant species of byproducts of histidine chlorination. When the iodide concentration was higher than  $2.5 \mu\text{M}$ , N-BOC-di-I-His was also produced at a relatively constant concentration, comparable to THMs and HAAs formed.

For the cumulative yields of THMs and HAAs, at  $0.5 \mu\text{M}$  of  $\text{I}^-$  condition, the production of N-BOC-I-His was approximately 1.33 times greater. As the iodide concentration increased, the difference became more extensive, and finally, it became 97.6 times greater at  $10 \mu\text{M}$  of  $\text{I}^-$ . The significantly higher formation of iodinated histidine products can be explained by the preferential reaction pathway of HOI. HOI preferentially acts as an iodination agent to cause iodination of histidine, and then acts as an oxidizing agent to decompose histidine to produce THM and HAA. Therefore, the chlorination of histidine in the presence of iodide will promote the formation of N-BOC-I-His than other DBPs such as THMs and HAAs. The total yield was sorted in decreasing order of iodinated histidine products > I-HAAs > I-THMs.

## Chapter 4. Conclusion

In this study, we found a new class of disinfection byproducts, iodinated imidazole products, resulting from the chlorine reaction of the imidazole compounds in the presence of iodide. During the reaction,  $I^-$  rapidly reacted with free chlorine to produce hypiodous acid (HOI), and this highly reactive iodine species was reacted with three model imidazole compounds: Imidazole-carboxylic acid, phenyl-imidazole-carboxylic acid, and histidine. We identified mono-iodinated and di-iodinated byproducts which have iodine linkage on the imidazole ring, and further tri-iodinated form was observed when more simple imidazole compound like imidazole-carboxylic acid was chlorinated. These compounds result from the rapid iodine addition, where the nitrogen atom of the anionic imidazole ring donates a lone pair to the electrophile. Subsequently, because of chemical stability, iodine addition is terminated by iodine substitution by releasing  $H^+$ .

This study has broadened our interest in the reactivity of histidine and the potential formation of iodinated histidine products in various chlorination conditions. Histidine is one of the representative compounds having imidazole moieties, and can be easily detected in natural water as a kind of amino acid. Hence, we focused on histidine chlorination in the presence of iodide. Unfortunately, iodinated histidine was not available as a standard for products. So, N-BOC-I-His and N-BOC-di-I-His were synthesized and prepared to determine the yield of iodinated histidine DBPs formed during chlorine reaction.

First, we focused on the kinetics study of how the presence of iodide during chlorination can influence the degradation of histidine and the formation of iodinated histidine products. The decomposition rate of histidine was accelerated in the order of the

presence of chlorine only, coexist of iodide, and bromide. On the other hand, the yield of iodinated histidine products was slightly decreased in the bromide condition. These results can be explained by the relative reactivity of HOI, HOBr, and HOCl to organic matter and the overall strength of the mixed oxidizing agents.

Second, experiments to assess the influences of various chlorination conditions on the histidine reactivity and iodinated histidine products formation were done in this study. In the chlorine dose effect, a high NaOCl dose limits the iodine substitution on the imidazole ring because it further oxidizes reactive iodine species (HOI) to non-reactive forms ( $\text{IO}_3^-$ ). On the other hand, as  $\text{I}^-$  concentrations increased, the amount of histidine decomposition and iodinated histidine products formation increased simultaneously. It is due to increasing reactive HOI which may induce the increasing chance of iodine substitution of histidine. As for the effect of  $\text{Br}^-/\text{I}^-$  molar ratio, at higher  $\text{Br}^-$  concentration, the iodinated histidine products were slightly less produced than only  $\text{I}^-$  containing conditions because of increasing in HOBr production that led to the relatively small proportion of HOI. But the concentration of histidine and these products remained constant regardless of bromide concentration. The pH of the solution played the most important role in the iodine substitution reaction. Generally, in the neutral or alkaline conditions, HOI (pKa 10.4) which is most reactive is the most predominant iodine species, as well as histidine (pKa 6.1) exists as an electron neutral molecule, acting as a highly reactive base for electrophiles. Thus, the pH affected the equilibrium of the reaction, and consequently, the concentration of iodinated histidine products formed was higher at a higher pH value.

Finally, a comparison of the yields of iodinated histidine products with THMs and HAAs formed simultaneously from the chlorination of histidine was conducted. In this study, the maximum total yield of THM and HAA was less than 0.4%, and rather, the overall yield

decreased as the iodide concentration increased. The dominant species of I-THMs and I-HAAs were iodoform (IF) and diiodoacetic acid (DIAA), respectively. Furthermore, at the highest iodide concentration in this experiment, the production of iodinated histidine products was 97.6 times higher than the cumulative yields of THMs and HAAs. It indicates in the chlorination of iodide-containing water, the iodination is promoted preferentially over the decomposition of histidine.

In conclusion, we confirmed that the imidazole ring could act as a precursor of iodinated disinfection byproducts, and these compounds were observed to be quite stable in the chlorinated water. It suggests that these imidazole DBPs have potential existence in the real chlorinated water. However, there were two limitations in this study.

Firstly, the possibility of occurrence of these iodinated imidazole DBPs in authentic chlorinated water was not confirmed. In actual water systems, the potential for iodination of imidazole is relatively low, either due to competitive effects with more organic substances or due to complex matrix. Also, even if these iodinated DBPs are generated, the concentration may be very small. Therefore, further toxicological studies are needed to prove that iodinated imidazole DBP is potent enough to explain the adverse health risks in order to prove that the discovery of this compound is meaningful even at low concentrations.

Second, the toxicity of these iodinated imidazole DBPs is unknown and further studies are needed for the reasons mentioned above. Often, cytotoxicity or genotoxicity assessments can be performed by applying oxidative stress to control cells or DNA and to determine  $IC_{25}$  or  $IC_{50}$  values. In addition, the relationship between compound structure and toxicity is characterized with respect to physicochemical properties including cellular uptake, metabolism



and intracellular interactions. Based on these toxicity data, a quantitative structure–activity relationship (QSAR) can be established. Therefore, further studies are needed to programmatically predict the toxicity of other compounds with imidazole functional groups through correlation analysis between imidazole structural parameters and derived IC<sub>50</sub> values.

# Reference

1. Dong, F.; Li, C.; He, G.; Chen, X.; Mao, X.; Kinetics and degradation pathway of sulfamethazine chlorination in pilot-scale water distribution systems. *Chemical Engineering Journal*, **2017**, 321, 521–532.
2. Zhang, T.; Xu, B.; Wang, A.; Cui, C.; Degradation kinetics of organic chloramines and formation of disinfection by-products during chlorination of creatinine. *Chemosphere*, **2018**, 195, 673–682.
3. Rook, J. J. Haloforms in drinking water. *Journal-American Water Works Association*, **1976**, 68(3), 168–172.
4. Shah, A. D.; Mitch, W. A.; Halonitroalkanes, halonitriles, haloamides, and N-nitrosamines: a critical review of nitrogenous disinfection byproduct formation pathways. *Environmental Science & Technology*, **2012**, 46(1), 119–131.
5. Krasner, S. W.; Weinberg, H. S.; Richardson, S. D.; Pastor, S. J.; Chinn, R.; Scrimanti, M. J.; ... ; Thruston, A. D.; Occurrence of a new generation of disinfection byproducts. *Environmental science & technology*, **2006**, 40(23), 7175–7185.
6. Jones, D.B.; Saglam, A.; Song, H.; Karanfil, T.; The impact of bromide/iodide concentration and ratio on iodinated trihalomethane formation and speciation. *Water research*, **2012**, 46(1), pp.11–20.
7. Plewa, M.J.; Wagner, E.D.; Richardson, S.D.; Thruston, A.D.; Woo, Y.T.; McKague, A.B.; Chemical and biological characterization of newly discovered iodoacid drinking water disinfection byproducts. *Environmental science & technology*, **2004**, 38(18), 4713–4722.
8. Richardson, S.D.; Fasano, F.; Ellington, J.J.; Crumley, F.G.; Buettner, K.M.; Evans, J.J.; Blount, B.C.; Silva, L.K.; Waite, T.J.; Luther, G.W.; McKague, A.B.; Occurrence and mammalian cell toxicity of iodinated disinfection byproducts in drinking

- water. *Environmental science & technology*, **2008**, 42(22), 8330–8338.
9. Wagner, E.D.; Plewa, M.J.; CHO cell cytotoxicity and genotoxicity analyses of disinfection by-products: an updated review. *Journal of Environmental Sciences*, **2017**, 58, 64–76.
  10. Liu, X.; Chen, L.; Yang, M.; Tan, C.; Chu, W.; The occurrence, characteristics, transformation and control of aromatic disinfection by-products: A review. *Water Research*, **2020**, 184, 116076.
  11. Hu, S.; Gong, T.; Wang, J.; Xian, Q.; Trihalomethane yields from twelve aromatic halogenated disinfection byproducts during chlor (am) ination. *Chemosphere*, **2019**, 228, 668–675.
  12. Ghosh, R.; Biplab, D; Review on: synthesis, chemistry and therapeutic approaches of imidazole derivatives. *ChemInform*, **2014**, 45(50)
  13. Pattison, D.I.; Davies, M.J.; Absolute rate constants for the reaction of hypochlorous acid with protein side chains and peptide bonds. *Chemical research in toxicology*, **2001**, 14(10), 1453–1464.
  14. Chen, T. H. Spectrophotometric determination of microquantities of chlorate, chlorite, hypochlorite and chloride in perchlorate. *Anal. Chem.*, **1967**, 39, 804–813.
  15. Bichsel, Y.; von Gunten, U. Oxidation of iodide and hypiodous acid in the disinfection of natural waters. *Environ. Sci. Technol.*, **1999**, 33, 4040–4045.
  16. Jiang, P.; Huang, G.; Jmaiff Blackstock. L.; Zhang. J.; Li, X.-F. Ascorbic acid assisted high performance liquid chromatography mass spectrometry differentiation of isomeric C-chloro- and N-chloro-tyrosyl peptides in water. *Anal. Chem.*, **2017**, 89(24), 13642–13650.
  17. Pearson, R. G.; Hard and soft acids and bases. *J. Am. Chem. Soc.*, **1963**, 85, 3533–3539.
  18. Edwards, J. O.; Pearson, R. G.; The factors determining nucleophilic reactivities. *J. Am. Chem. Soc.*, **1962**, 84, 16.

19. Munch, D. J.; Hautman, D. P.; Method 551.1: Determination of chlorination disinfection byproducts, chlorinated solvents, and halogenated pesticides/herbicides in drinking water by liquid–liquid extraction and gas chromatography with electron–capture detection. *Methods for the Determination of organic compounds in drinking water.*, **1995**.
20. Hodgeson, J. W.; Collins, J.; Barth, R. E.; Munch, D.; Munch, J.; Pawlecki, A.; METHOD 552.2 Determination of haloacetic acids and dalapon in drinking water by liquid–liquid extraction, derivatization and gas chromatography with electron capture detection. *US Environmental Protection Agency, Cincinnati.*, **1995**.
21. Brunings, K. J. Preparation and properties of the iodohistidines. *J. Am. Chem. Soc.*, **1947**, 69, 2, 205–208.
22. Li, C. H. Kinetics of reactions between iodine and histidine. *J. Am. Chem. Soc.*, **1944**, 66, 225–230
23. Li, C.; Gao, N.; Chu, W.; Bond, T.; Wei, X.; Comparison of THMs and HANs formation potential from the chlorination of free and combined histidine and glycine. *Chemical Engineering Journal*, **2017**, 307, 487–495.
24. Han, Y.; Zhou, Y.; Liu, Y. D.; Zhong, R.; Reaction Mechanisms of Histidine and Carnosine with Hypochlorous Acid Along with Chlorination Reactivity of N–Chlorinated Intermediates: A Computational Study. *Chemical Research in Toxicology*, **2022**, 35(5), 750–759.
25. Huang, G.; Jiang, P.; Li, X.–F. Mass spectrometry identification of N–chlorinated dipeptides in drinking water. *Anal. Chem.*, **2017**, 89(7), 4204–4209.
26. Pattison, D. I.; Davies, M. J. Absolute rate constants for the reaction of hypochlorous acid with protein side chains and peptide bonds. *Chem. Res. Toxicol.*, **2001**, 14, 1453–1464.
27. Bichsel, Y.; von Gunten, U.; Oxidation of iodide and hypiodous acid in the disinfection of natural waters. *Environ. Sci. Technol.*, **1999**, 33(22), 4040–4045.

28. Nagy, J.C.; Kumar, K.; Margerum, D.W.; Nonmetal redox kinetics: oxidation of iodide by hypochlorous acid and by nitrogen trichloride measured by the pulsed–accelerated–flow method. *Inorganic Chemistry*, **1988**, 27(16), 2773–2780.
29. Rose, M. R.; Lau, S. S.; Prasse, C.; Sivey, J. D.; Exotic electrophiles in chlorinated and chloraminated water: When conventional kinetic models and reaction pathways fall short. *Environmental Science & Technology Letters*, **2020**, 7(6), 360–370.
30. Guo, G.; Chen, X. Halogenating reaction activity of aromatic organic compounds during disinfection of drinking water. *Journal of hazardous materials*, **2009**, 163(2–3), 1207–1212.
31. Vikesland, P. J.; Fiss, E. M.; Wigginton, K. R.; McNeill, K.; Arnold, W. A.; Halogenation of bisphenol–A, triclosan, and phenols in chlorinated waters containing iodide. *Environmental science & technology*, **2013**, 47(13), 6764–6772.
32. Gallard, H.; Pellizzari, F.; Croue, J. P.; Legube, B.; Rate constants of reactions of bromine with phenols in aqueous solution. *Water research*, **2003**, 37(12), 2883–2892.
33. Richardson, S.D.; Fasano, F.; Ellington, J.J.; Crumley, F.G.; Buettner, K.M.; Evans, J.J.; Blount, B.C.; Silva, L.K.; Waite, T.J.; Luther, G.W.; McKague, A.B.; Occurrence and mammalian cell toxicity of iodinated disinfection byproducts in drinking water. *Environmental science & technology*, **2008**, 42(22), 8330–8338.
34. Smith, E. M.; Plewa, M. J.; Lindell, C. L.; Richardson, S. D.; Mitch, W. A.; Comparison of byproduct formation in waters treated with chlorine and iodine: relevance to point–of–use–treatment. *Environmental Science & Technology*, **2010**, 44(22), 8446–8452.
35. Hureiki, L.; Croué, J.P.; Legube, B.; Chlorination studies of free and combined amino acids. *Water Research*, **1994**, 2521–2531.
36. Scully, F. E.; Kravitz, R.; Howell, G. D.; Speed, M. A.; Arber, R. P.; Contribution of proteins to the formation of trihalomethanes

- on chlorination of natural water. *Water Chlorination: Environmental Impact and Health Effects*, **1985**, 5, 807–820.
37. Liu, S.; Li, Z.; Dong, H.; Goodman, B. A.; Qiang, Z.; Formation of iodo-trihalomethanes, iodo-acetic acids, and iodo-acetamides during chloramination of iodide-containing waters: factors influencing formation and reaction pathways. *Journal of hazardous materials*, **2017**, 321, 28–36.
  38. Duirk, S. E., Lindell, C., Cornelison, C. C., Kormos, J., Ternes, T. A., Attene-Ramos, M., ... & Richardson, S. D.; Formation of toxic iodinated disinfection by-products from compounds used in medical imaging. *Environmental science & technology*, **2011**, 45(16), 6845–6854.
  39. Dong, H., Qiang, Z., & Richardson, S. D.; Formation of iodinated disinfection byproducts (I-DBPs) in drinking water: emerging concerns and current issues. *Accounts of Chemical Research*, **2019**, 52(4), 896–905.
  40. Plewa, M. J., Wagner, E. D., & Richardson, S. D.; TIC-Tox: A preliminary discussion on identifying the forcing agents of DBP-mediated toxicity of disinfected water. *Journal of Environmental Sciences*, **2017**, 58, 208–216.
  41. Ding, G., & Zhang, X.; A picture of polar iodinated disinfection byproducts in drinking water by (UPLC/) ESI-tqMS. *Environmental science & technology*, **2009**, 43(24), 9287–9293.
  42. Plewa, M. J., Wagner, E. D., Muellner, M. G., Hsu, K. M., & Richardson, S. D.; Comparative mammalian cell toxicity of N-DBPs and C-DBPs. *Disinfection By-Products in Drinking water*, **2008**, chapter 3, 36–50
  43. Woo, B., Park, J. H., Kim, S., Lee, J., Choi, J. H., & Pyo, H.; Determination of six iodotrihalomethanes in drinking water in Korea. *Science of the Total Environment*, **2018**, 640, 581–590.

## 국문초록

이미다졸은 종종 생물학적 물질 (예: 히스티딘, 히스타민 및 핵산)의 구성성분으로 식수원에서 발견되며, 약품 및 살충제와 같은 인공 화학물질에서도 발견된다. 이미다졸은 극성 방향족 화합물로서, 할로젠화 가능성이 높기 때문에 요오드화 소독부산물 (I-DBPs)의 중요한 전구체가 될 수 있다. 음용수에서 I-DBPs의 형성은 Cl- 및 Br-DBPs에 비해 높은 독성으로 인해 우려가 증가함에 따라 이러한 가능성을 조사할 필요가 있다.

이 연구는 이미다졸 고리를 포함하는 세 가지 유기 화합물인 이미다졸-카르복실산, 페닐-이미다졸-카르복실산 및 히스티딘으로부터 요오드화된 이미다졸 소독부산물의 형성 가능성을 확인하기 위해 수행되었다. 액체 크로마토그래피 질량 분석 (LC-MS)을 사용하여, 요오드화 이미다졸 소독부산물이 실험실 모의 염소화수에서 검출되었으며, 그들의 구조 또한 제안되었다. 이미다졸-카르복실산은 디-I- 및 트리-I-이미다졸을 생성하였고, 페닐-이미다졸-카르복실산은 요오드 치환이 벤젠 고리에서 발생한 것으로 추정되는 모노-I- 및 디-I-페닐-이미다졸을 형성하였다. 히스티딘은 자유 아민 그룹을 친전자성 반응에 불활성화하기 위하여 N-터트-부틸옥시카르보닐 보호기 (N-BOC 그룹)에 보호된 형태로 수행되었다. N-BOC-히스티딘은 N-BOC-I- 및 N-BOC-디-I-히스티딘을 생성하였다.

우리는 히스티딘으로부터 형성된 지배적인 요오드화된 소독부산물에 초점을 맞추었다. 요오드화된 히스티딘 화합물에 대해, 우리는 이들 화합물을 합성하여 수율을 정량했다. 이 연구는 히스티딘이 염소만 존재하는 것보다 요오드가 존재하는 염소화 동안 더 반응성이 있음을 입증했다. 히스티딘의 분해 및 요오드화 소독부산물의 형성에 대해 차아염소산 투여량과 같은 소독 조건과 pH, 요오드 이온 및 브롬 이온 등의 물 조건의 영향도 특성화되었다. 더 낮은 차아염소산 투여량, 브롬 이온/요오드 이온 비율 및 더 높은 요오드 이온 농도에서, 히스티딘의 많은 분해와 요오드화된 히스티딘 생성물의 높은 형성이 발생되었다.

요오드화 소독부산물의 수율은 용액 pH에 크게 영향을 받았다. 알칼리성 조건에서 높은 농도의 요오드화된 히스티딘 소독부산물이 생성되었다. 마지막으로, 우리는 히스티딘의 염소화로부터 동시에 형성된 트리할로메탄 및 할로아세트산과 요오드화된 히스티딘 소독부산물의 수율을 비교하였다. 트리할로메탄과 할로아세트산의 최대 총 수율은 0.4% 미만이었으며, 요오드화 히스티딘 생성물의 수율 (최대 ~5.5%)에 비해 매우 작았다. 이러한 발견은 요오드화 히스티딘 화합물의 형태가 현재 규제되고 있는 트리할로메탄 또는 할로아세트산보다 생산량 측면에서 더 중요한 역할을 할 수 있음을 뒷받침한다. 그러나 이에 대한 증거는 이러한 화합물의 구조 및 역학에 대한 추가 독성학적 연구에 의해 뒷받침되어야 한다.

**Keyword :** 염소 소독; 요오드 이온; 이미다졸; 히스티딘; 소독부산물;  
**Student Number :** 2020-27348